THE TRANSITION FROM THE ANNULAR TO THE SLUG FLOW REGIME IN TWO-PHASE FLOW

Robert D. Haberstroh
Peter Griffith

June 1964

Technical Report 5003-28
Department of
Mechanical Engineering
Massachusetts Institute
of Technology

Contract No. AT(30-1)-3301

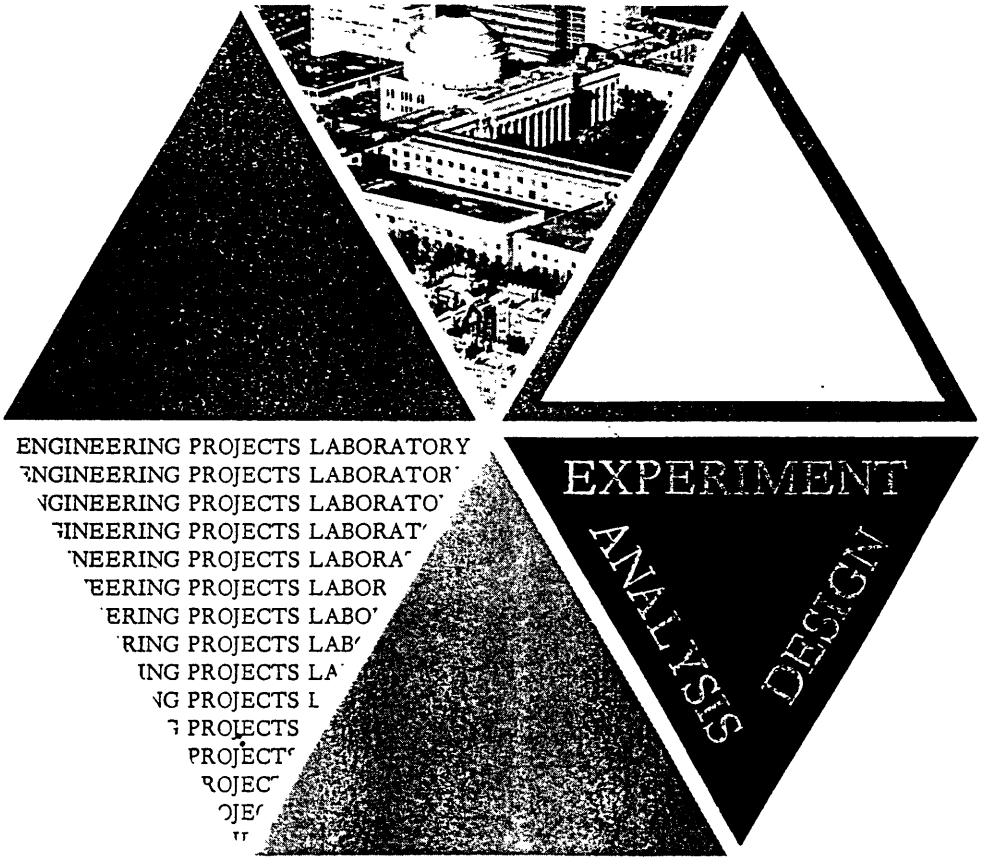

TECHNICAL REPORT 5003-28

THE TRANSITION FROM THE ANNULAR TO THE SLUG FLOW REGIME IN TWO-PHASE FLOW

by

Robert D. Haberstroh*

and

Peter Griffith**

for

THE ATOMIC ENERGY COMMISSION

Contract No. AT(30-1)-3301

DSR No. 5003

Division of Sponsored Research

Massachusetts Institute of Technology

Cambridge 39, Massachusetts

* Instructor, Mechanical Engineering, M.I.T. Present Address
Associate Professor, Department of Mechanical Engineering
Colorado State University, Ft. Collins, Colorado

** Associate Professor of Mechanical Engineering, M.I.T.

ABSTRACT

Experiments were conducted to determine the transition from annular to semiannular flow regimes for two-phase, gas-liquid upflow in vertical tubes. The influences of liquid flow rate, tube diameter, liquid viscosity, surface tension, and density ratio were tested.

The transition location, giving the least gas flow which will support annular flow, is correlated for low liquid flows. The effects of surface tension and liquid viscosity are small for tubes of 0.5" and greater diameter. For large liquid flows the transition occurs at constant quality. Over the range of variables tested, the void fraction at transition lies between 80% and 90%. The criterion of transition is the appearance of liquid plugs which intermittently bridge across the tube.

The pressure drop and volume void fraction at transition are reported but not correlated. Recommendations for extension of the experimental results to untested conditions are presented.

ACKNOWLEDGMENTS

This work has been sponsored by the Atomic Energy Commision. It has been performed at Massachusetts Institute of Technology in the Engineering Projects Laboratory and in the Heat Transfer Laboratory, which is under the direction of Warren M. Rohsenow.

TABLE OF CONTENTS

1.1. A Design Problem

The designer of two-phase heat- and mass-transfer equipment faces the problem of sizing the tubes and flow passages within his preordained limits of pressure drop and heat transfer rate. With knowledge of the fluid properties he must thus be able to predict the pressure drop per unit length of a given-size passage, knowing the quantities of fluids moving. He must also be able to make calculations from similar inputs to compute the heat transfer rate per unit area. The pressure drop, being a variable which is measurable in the simpler two-phase flows (those without heat transfer), received attention from the earlier engineering investigators. A widely used correlation for pressure drop is that of Lockhart and Martinelli[1]*, who expressed two-phase pressure drop by analogy to single-phase flow in pipes, which is well understood. They did not distinguish among various possible gas-liquid geometric distributions, with the outcome that their results cannot be applied over all possible ranges of gas and liquid flow rates in a given-size pipe; the correlation is reasonably satisfactory for some geometries but badly in error for others. Thus before the designer can make use of such data he must by other means determine whether the flow geometry will be appropriate to the pressure drop correlation used. The purpose of this

---

* Numbers in parenthesis, thus: (1), in the text designate references listed in the Bibliography.

paper is to provide means of determining the geometric nature of the flow as a preliminary to the designer's estimate of pressure drop and (eventually) heat transfer rate.

1.2. Problem Statement: The Prediction of Flow Regimes

The various geometric arrangements are referred to as flow regimes. These regimes, which are discussed in some detail in the next chapter, have been called by a variety of names, with varying degrees of fine distinction among geometric differences. There are differences between the flow regimes found in vertical pipes and those found in horizontal pipes; since attention is presently concentrated on vertical tubes, the horizontal-flow regimes will not be listed.

In vertical tubes, one can imagine an upward flow of liquid (single-phase). If a very small quantity of gas is injected at the bottom while the liquid flow continues, individual gas bubbles will rise through and with the liquid, giving "bubbly flow." Maintaining the liquid flow but increasing the gas flow causes the appearance of more gas bubbles until the bubbles begin to touch one another and agglomerate. Continuing to increase the gas flow gives rise to "slug flow," in which the agglomerated bubbles form stable, bullet-shaped bubbles of gas separated by "slugs" of liquid. Further increase of the gas flow destroys the stability of the bubbles, producing "churn flow" or

"semiannular flow," in which slugs of liquid separate adjacent gas bubbles only temporarily; the slugs are violently blasted upward by the gas pressure behind them, then they dissipate into an annular wall film or strike and join other slugs of liquid. Still further increase of gas flow "blows out" the slugs of liquid, leaving a continuous core of gas near the middle of the tube and an annulus of liquid on the wall; this geometry is called "annular flow." If the gas flow is high enough to tear droplets of liquid from waves on the interfacial surface of the annular film, a substantial part of the liquid flow can be due to "spray" or "mist." It is conceivable that in a long tube where boiling is taking place, beginning with all liquid at the bottom, all of these flow regimes might appear within the length of the tube, since the quantity of gas flowing can increase along this length.

With such a variety of possible flow regimes and with the inevitable interaction between the flow regime and flow dynamics, it is necessary to determine what flow regime will occur for given input conditions to a given pipe. A controlled experiment can be used to obtain this information, and in the present experiments complicating factors are removed by the elimination of heat transfer and phase change. These effects are avoided by use of two-phase two-component flow where the components are virtually immiscible. Further, attention is restricted to two regimes of practical interest, slug flow and annular flow. In fact the regime of semiannular

flow lies between the two, and the semiannular regime bears many similarities to slug flow. The transition between these two regimes will not be treated except in a descriptive way. The presence of spray droplets in the gas core adds a new complicaiton which will be treated later. A correct theory of all possible transitions would have to represent the intersections of theories for each of these flow regimes, but suitable theories are lacking for all but one (slug flow) of the regimes of interest, and even this one is not complete. Thus, although a theoretical matching of adjacent regimes would provide an ideal means of defining the regime boundaries, the absence of theories makes that procedure impossible.

The observer of flow regimes is thus forced to adopt a phenomonological definition of the transitions between regimes which he can distinguish only by experimentally observed differences. As a number of flow parameters can be observed, the choice of the distinguishing parameter becomes arbitrary. The parameter chosen here is the geometry of the liquid-gas combination, as will be discussed later. Also, the fact that there are two transitions between slug flow and annular flow requires a statement as to which of the two is being studied. This paper concentrates on the lower-gas-flow limit of annular flow.

The independent variables are usually the flow rates of liquid and gas, the fluid properties, and the pipe diameter;

the result one desires is a simple statement which permits a decision as to whether annular flow or another regime will persist for given upflow rates of given liquid and gas through a vertical tube of a certain size. For analytical purposes this goal is restated to ask the equivalent question, "What is the least gas velocity which will support annular flow, given the tube size, fluid properties, and liquid flow rate?"

1.3. Prediction of Voids in Slug Flow

For the regime of stable slug flow there is a theory which permits computing the void fraction. Slug flow was studied by Griffith and Wallis[2], who presented a means of computing the average density which would lead to the void in vertical tubes 1/2 inch and larger in diameter. Their results were extended and modified by Nicklin, Wilkes, and Davidson[3], who showed that the bubble rise velocity can be expressed as the sum of the rise velocity in still liquid plus a term which is 1.2 times the average liquid velocity. The factor of 1.2 is associated with a turbulent, fully-developed velocity profile, where the centerline liquid velocity is 1.2 times the average. This result allows computations of the void fraction by insertion of the continuity equation, leaving the void

$$\alpha = \frac{V_{g_s}}{1.2(V_{f_s} + V_{g_s}) + 0.35\sqrt{gD}}. \qquad (1)$$

According to this result the void can never exceed 83.3% for slug flow which produces upflow of liquid. It is interesting to note that this description of slug flow is complete without reference to the densities of the fluids; the relation among void, liquid flow, and gas flow is determined by geometric conditions alone if the fully developed velocity profile condition is met. The geometries of slug flow and other regimes are sketched in Figure 1.

Nicklin and Davidson[4] proceeded to obtain the upper limit of gas flow for stable slug flow, i.e., the transition to semiannular flow, for low liquid flows. They found the mechanism of transition to be the same as that of "flooding" in counterflow wetted-wall columns; in this case the falling liquid film and the rising bubble constituted the components of the wetted-wall column. They obtained a result for zero liquid flow which confirmed their experiment in the particular pipe (1.02" diameter) they used, but they did not extend their results to other pipes or fluids. They found that the flooding calculation did not predict the departure from slug flow for large liquid flows, and they speculated that another mechanism was involved.

Slug flows in small-bore tubes were studied by Suo[5]. He found that geometry alone was insufficient to determine the void in capillary slug flow. The liquid properties are important, particularly the viscosity and surface tension. But he found that if the liquid flow is great enough to be considered turbulent, the void fraction when the bubbles touch

each other (breakup of slug flow to annular flow) is 84%, which to the precision possible in flow regime studies is very close to the 83.3% of reference (3).

The use of Eq. (1) to predict the void in unstable slug flow (or semiannular flow) is fairly successful (3) near the lower limit of unstable slug flow, but it is increasingly inaccurate as the gas velocity is increased. The limitation of void to 83.3% for upflow makes this theory unsuitable for the region of interest, namely, the onset of unstable slug flow from annular flow, since the experimental results give transition voids in some cases well over 83.3%.

1.4. Prediction of Voids in Annular Flow

If, for a given liquid velocity, the gas velocity is sufficiently high, the gas becomes the continuous phase, and the liquid is distributed in a film upon the tube wall. The interface between liquid and gas is rough; the roughness consists of surface waves which individually may move either up or down. Visually, the waves fall into two categories. If the liquid flow is extremely small, the wall film thickness is small (high void fraction), and the surface waves take the form of symmetrical rings which move slowly (at much less than gas velocity) upward with constant velocity and more or less regular spacing. Occasionally slightly larger waves, moving more rapidly, overtake the average-size waves, giving the impression of a "group-velocity" effect. The interface has a glassy appearance. The void

fraction for this flow is very high, about 95% or more in air-water systems, and usually a slight increase in the air flow will give rise to dry spots on the tube wall. This geometry is sketched in Figure 1e.

The more common geometry is that of an extremely rough film with waves of irregular shape moving along the interface. The velocity of the waves is far from constant, giving surges in the liquid velocity which become increasingly pronounced as the gas velocity is reduced and the void fraction decreases. The waves may account for a large part or all of the liquid flow; under some conditions one can observe that the thin film between waves is stationary or even downward-moving. Small gas bubbles are often entrained in the liquid film. The interface is by no means glassy; it has a stippled appearance. This flow is sketched in Figure 1f.

A completely satisfactory theory of annular flow would permit calculation of the void and pressure drop for any liquid and gas flow rate. A number of investigators have undertaken development of such a theory, but none has been completely successful, mainly because of the difficulty of characterizing the conditions at the moving interface. Various means have been tried to account for the interface shape or to avoid need to consider it, and in general the more successful efforts have followed the latter course. One researcher, however, who attempted to account in some way for the interface roughness and wave motion was Laird[6].

He used a physical model consisting of a wall film with a sinusoidal surface; both fluids were in laminar flow. His intention was to establish limits of stability for the sinusoidal surface, but he was unable to solve the Navier-Stokes equations which were the starting point for his analysis. Laird's modelling of the annular interface with a sine wave seems a reasonable simplification of the actual flow, but his inability to complete a theory for the simple laminar-laminar flow combination is not encouraging to the investigator who desires solutions to the more practical case where both fluids are turbulent. Laird's experiments were very interesting; he modelled the time-varying interface experimentally by means of a hydraulically-driven rubber diaphragm and obtained gas pressure drops in the dry model whcih were comparable with the high pressure drops in annular two-phase flow.

Various investigations have analyzed annular flows in which the interface was considered smooth, the liquid flow was either laminar or turbulent with a Karman universal velocity profile, and the gas flow was either laminar or turbulent with a friction factor to be determined at the interface. For applications to engineering-size pipes and flow rates, the studies involving laminar flow suffered from lack of realism in that they predict heavy dependence on the fluid viscosities. The turbulent analyses always needed experiments for friction factors.

One important analysis which touches upon this group is that of Calvert and Williams[7], who worked with a tur-

bulent wall film but concluded that the universal velocity profile is inappropriate because the distribution of apparent shear stress in the film is different from that in single-phase flow. They computed the shear stress distribution from a one-dimensional momentum analysis and found it to be linear for a thin film, but with a discontinuity of slope at the gas-liquid interface. Thus in general the shear in the film would not go to zero if extended to the tube centerline, as the shear in single-phase flow does. They used the mixing-length theory to relate the apparent shear stress to the velocity gradient and integrated once to obtain the velocity profile and agin to get the total liquid flow in the film. From their theory, given the pressure drop and liquid flow, one can correctly predict the void fraction in annular flow.

The difficulty is that the pressure drop is a variable dependent on liquid and gas flow, so a relation between pressure drop (or interfacial shear, which Calvert and Williams actually used) and gas flow is needed to complete the relationship among the liquid flow, gas flow, and void. They obtained this relation by experiments with air and water to obtain a drag coefficient for the interface. They made an unfortunate choice in dividing the drag coefficient into two parts, one due to friction at the wall of a smooth, dry tube, and the other due to the rough profile of the interface; the physics of the interfacial drag is only remotely related to the smooth, dry tube, but they were successful because the profile drag is huge compared with the other term.

The Calvert and Williams results are especially interesting because they contain a possible criterion for a transition away from annular flow. For a given interfacial shear stress and liquid flow there are two solutions for the void fraction in the Calvert and Williams theory. If the void exceeds the void at the least interfacial shear which would drive the given liquid flow, annular flow is possible; if not, annular flow is impossible. Thus only one of the solutions represents stable annular flow, and the transition line is the locus of minimum interfacial shear stress. This criterion coincides with the minimum-pressure-drop criterion applied to experimental data by Govier, Radford, and Dunn[8]. Their criterion, based on visual observation of the flow through transparent-wall tubes, is as arbitrary as the one used in the present experiments, which is based on geometric changes. Thus one would expect to find, and does find, that the two criteria give two different locations for the lower limit of annular flow. When the Calvert and Williams theory is plotted with the present data, the two transition lines cross each other at an angle which is not small.

A comprehensive review of these works and others up to about 1958 is given by Charvonia[9].

An entirely different approach was taken by Wallis[10], who studied the flooding or catastrophic instability of countercurrent gas-liquid flows in vertical tubes from the

same point of view used by others to examine similar phenomena in packed columns. He simplified the earlier results to get the equation of the flooding line for the packed columns,

$$V_{f_d}^{*1/2} + V_g^{*1/2} = 0.775, \qquad (2)$$

where the subscript d indicates that downflow of the liquid is taken as positive. The flooding line divides possible counterflow operation from impossible counterflow; if the left-hand side of Eq. (2) exceeds 0.775, stable operation is impossible. Wallis's definitions of the superficial velocities, if the gas is much less dense thant the liquid, reduce to

$$V_g^* \equiv \frac{V_{g_s}}{\sqrt{\frac{\rho_f}{\rho_g}}\sqrt{gD}} = \frac{Q_g}{A\sqrt{\frac{\rho_f}{\rho_g}}\sqrt{gD}} \qquad (3)$$

and

$$V_f^* \equiv \frac{V_{f_s}}{\sqrt{gD}} = \frac{Q_f}{A\sqrt{gD}}, \qquad (4)$$

where for the packed towers D is a characteristic dimension based on the ratio of volume to surface area. Wallis then made flooding experiments with air and water in vertical tubes, let D stand for the pipe diameter, and successfuly correlated the pipe flooding data with Eq. (2).

He found that the constant, 0.775, in Eq. (2) actually varied from pipe to pipe, depending on entrance and exit conditions, but the usefulness of the correlating parameters V_f^* and V_g^* was unimpaired by such changes.

Wallis then reasoned[11] that there is a connection between countercurrent flooding and transition from annular to semiannular cocurrent upflow, at least at zero liquid flow, where the two phenomena should coincide. On the basis of experiments in which he admitted water through a porous inlet partway along a tube in which air flowed upward, permitting the water to flow in either direction and eliminating a problem of entrance design, he concluded that the boundary between possible and impossible annular upflow is represented by a constant value of gas flow $0.8 < V_g^* < 0.9$. He successfully compared this result with the results of other investigators for very small liquid flows. At the time the constant-gas-flow transition was thought to be suitable for larger liquid flows as well, but improved means of observing the flow patterns have indicated that this is not so, and the result of Reference (11) is correctly applied only at zero liquid flow.

Having thus made a connection between flooding in countercurrent systems and annular flow in cocurrent systems, Wallis et al.[12] were encouraged to attempt to correlate void fraction with phase flow rates for annular flow by use of the same parameters V_g^* and V_f^*. A successful correlation

by use of these groups would have the advantage of having jumped over the problem of characterizing the undetermined interface shape and avoiding the need to study pressure drop or interfacial shear as a necessary part of the void fraction study. They succeeded in doing that, and their result takes the form

$$\frac{V_g^*}{1 - 2.85(1 - \alpha)} - \frac{V_f^*}{2.85(1 - \alpha)} = 0.775, \qquad (5)$$

They compare this correlation with their own data and with data of others and indicate good agreement. These investigators also present another criterion of transition, namely, the onset of inconsistency in void measurements for fixed phase flow rates. They indicate that this transition takes place at about 80% void fraction, and they show a curve which displays the scatter of the void data for a certain value of V_f^* as well as plots of Eq.'s (1) and (5), showing an intersection of these two theories at about 80% void. Pressure drop data are presented but are not as yet correlated.

Equation (5) summarizes the only theory of annular flow which bypasses the need to fix the pressure drop in order to predict the void fraction. It gives results for the void which compare rather closely with the experiments described in this report, but the extreme sensitivity of the liquid fraction to small changes of void at high values of demands greater precision for transition prediction

than Eq. (5) can give. The experiments illustrate this; Eq. (5) comes close but does not quite fit the experimental results for annular flow in tubes whose diameter differs from 1.0".

There are thus two methods of calculating the void in the region of interest, Eq. (1) arising from slug flow theory and Eq. (5) arising from annular flow studies. Eq. (1) is inappropriate, and Eq. (5) is insufficiently accurate to predict the transition.

1.5. Annular Flow with Spray

If the annular wall film is rough enough and the gas velocity is sufficiently high, liquid can be sheared from the crests of the waves, giving rise to the transport of liquid in the form of spray carried by the gas core. In a long tube a steady state is reached between the stripping of the wave tops and redeposition of droplets on the wave slopes as "rain," so there is an apparently steady net delivery of liquid to the pipe exit by means of spray. A sketch of this sort of flow would be identical to one for rough-film annular flow but with addition of some dots to represent droplets of liquid in the gas core; no sketch is shown.

In 1962, Wallis[13] studied the question of the lowest gas velocity which produces spray in an annular flow. He found that over a limited range of pipe sizes and liquid flow rates, for cocurrent upflow or downflow, the critical gas velocity is about 70 or 75 fps, though it tends to increase somewhat with decreasing pipe diameter. He suggested

that a critical value of the Weber Number,

$$(We) = \frac{V_{g_s}^2 \rho_g D}{g_c \sigma} , \qquad (6)$$

might be useful for predicting the onset of spray. His work on spray continues, however, and he has been obtaining and interpreting data (12, 14) for larger size tubes with cocurrent upflow and downflow without reference to his earlier Weber Number criterion. The spray-annular regime is thus as yet without a theory, but it is under attack by Wallis; the regime is mentioned here because it appears to be importantly involved in the transitions to be discussed later.

1.6. Transitions from Annular Flow to Adjacent Regimes

In order for one to describe a transition, a definition of transition is needed, and for present purposes the geometric definition will be used: A transition has occurred when the geometry of the gas-liquid distribution has changed. This definition is not likely to give the same results as the minimum-interfacial-shear criterion of references (7) and (8) or the deviant-void-fraction criterion of reference (12). The geometric definition has the advantages that it notes a difference which significantly influences the flow dynamics and that it is directly measurable with the help of suitable tools without dependence on a questionable annular-flow theory. Although minima of pressure drop do occur, experiments indicate that the geometry is that of semiannular

flow carrying numerous and long plugs of liquid, especially at the higher liquid flows; that is, the pressure drop minimum occurs when semiannular flow is already well established geometrically. It is also true that the void fraction measurements are inconsistent for semiannular flow, but the irregular surging of large waves in the lower regions of annular flow also causes deviations in the measured void in that regime.

It is characteristic of the transitions from annular flow to adjacent regimes that the changes are gradual. There are no sharp breaks in values of pressure drop or void, with the result that the "transition lines" are really broad bands which divide a region definitely representing one regime from a region certainly showing another. To specify the locations of such bands, however, it is convenient to try to pass a single line through the center of the region of uncertainty, and this is what is done in Figure 2, which roughly locates the several regimes in question on the usual coordinates of a "flow map," Q_g vs. Q_f or V_{g_s} vs. V_{f_s}. The present experiments establish the shape of the line which divides the annular and spray regimes (taken together) from the semiannular; that is, the line which divides regimes where the gas is the continuous phase from the regime where the liquid is continuous. As will be indicated, the annular-semiannular boundary is emphasized, and the data are merely reported for the spray-semiannular boundary.

2. MODEL FOR ANNULAR FLOW AND TRANSITION

2.1. Choice of Model

As has been suggested in the review of annular flow, the choice of physical models is limited by realism on one hand and tractability on the other. There is little point, though, in attempting to use a complicated model when, as in the present situtation, the mechanism of momentun transport is not entirely clear. Thus one should use the simplest physical model which displays the effects visible in experiments. The model should not demand attention to fine points of the flow, such as the details of the unsteady motion of the interface, if it is to be used to predict the gross behavior of a long tube. The literature contains curves for the slug-annular transition which for given fluids in given tubes slope upward, downward, or horizontally with increasing liquid flow. The present mission is in part to establish which of these slopes is correct, and the model need be no more sophisticated than is necessary to resolve the question.

An annular flow model is being studied for transition for two reasons. One is the transition is found to occur in a small range of void fractions (Figures 24 and 24a) most of which are above that which can be predicted with a slug flow expression Eq. (1). The second reason is, if one picks a void for transition and substitutes it into Eq. (1) to get the volume flow rates for transition, one finds that the volume flow ratio at transition is independent of the vapor

properties. The data of Figure 23 show this is not the case at all.

With these ideas in mind, let the model of annular flow consist of a length of smooth tubing containing an annulus of liquid whose inner surface is wavy or rough, as in Figure 3. The interface is rough, and it is moving, but the essential feature is that the motion of the interface is characterized by a single velocity which is constant in time. This implies that the length of tube examined is great enough to permit averaging along the length at an instant, and that means of measuring the velocities is to average them over a period of time.

Before proceeding with the treatment of this model, it would be well to recall the criterion of transition, namely, the change in interfacial geometry from one of continuous gas to one of discontinuous gas. The simplified model at the outset does not include any direct statement about this change, and it is necessary to provide some connection between the model and the geometry change. This connection is provided by part of the experimental results; the transition was found to occur at void fractions which are bounded by rather narrow limits, and the void at transition is the same for the three pipe diameters used in the tests. This is the transition criterion.

2.2. Assumptions

To simplify the analysis, it is necessary to make some assumptions. First, assume that the flow is steady, one-

dimensional, and fully developed, so the continuity equation becomes trivial, the flow quantities become the time averages mentioned above, and the location along the pipe where the analysis is made does not affect the result. There is also no radial pressure gradient. Assume that the gas is imcompressible in the sense that its velocity is much less than the sonic velocity. In fact the low-pressure air experiments involve rather substantial changes in the air density due to decreasing pressure as the air moves downstream. Let the length of the model control volume be short enough to permit ignoring this variation. Assume that the gas density is much less than the liquid density; this is appropriate in the range of variables tested and is not greatly in error at moderate pressures in steam-water systems. This assumption is not absolutely essential, but it is a matter of convenience as it eliminates the need to account for gravity pressure gradient in the gas. Both gas and liquid flows are assumed to be turbulent, so their viscosities will be relatively unimportant. The surface tension between gas and liquid will be ignored; presumably if the pipes are sufficiently large this assumption will be correct. These assumptions can be checked in the course of the experiments.

2.3. Analysis

The forces which remain for the gas due to the pressure and the interfacial shear. For the liquid the forces are due to pressure, interfacial shear, wall shear, and gravity.

Using the expression (-dp/dz) to denote the pressure drop of the entire tube divided by the tube length, one writes the momentum equation for the gas as

$$(-\frac{dp}{dz}) = \frac{2\tau_i}{r_i} = \frac{2\tau_i}{r_o\sqrt{\alpha}} . \tag{7}$$

The liquid momentum equation gives

$$\tau_o = \tau_i \frac{r_i}{r_o} + [(-\frac{dp}{dz} - \rho_f \frac{g}{g_c}] \frac{r_o}{2} (1 - \frac{r_i^2}{r_o^2})$$

or

$$\tau_o = \tau_i\sqrt{\alpha} + [(-\frac{dp}{dz}) - \rho_f \frac{g}{g_c}] \frac{r_o}{2} (1 - \alpha) \tag{8}$$

Define the friction factor at the interface as

$$f_i \equiv \frac{\tau_i}{\frac{\rho_g}{2g_c} (V_g - V_{g_i})^2} \tag{9}$$

and at the wall as

$$f_o \equiv \frac{\tau_o}{\frac{\rho_f}{2g_c} V_f^2} . \tag{10}$$

Now eliminate (-dp/dz) from (7) and (8) and insert (9) and (10), leaving

$$(V_g - V_{g_i})^2 = \frac{\rho_f}{\rho_g} \left[\sqrt{\alpha} \frac{f_i}{f_o} V_f^2 + \frac{\sqrt{\alpha}\ (1-\alpha)}{2\ f_i} gD \right] . \tag{11}$$

(interface shear) (wall shear) (gravity)

In terms of the superficial velocities, defined as

$$V_{g_s} \equiv \frac{Q_g}{A} = \alpha V_g \quad \text{and} \quad V_{f_s} \equiv \frac{Q_f}{A} = (1-\alpha)\ V_f,$$

$$V_{g_s} = \alpha V_{g_i} + \sqrt{\frac{\rho_f}{\rho_g}} \sqrt{\frac{\alpha^{5/2} f_o}{(1-\alpha)^2 f_i} V_{f_s}^2 + \frac{\alpha^{5/2}(1-\alpha)}{2 f_i} gD}. \qquad (12)$$

(interface shear) (wall shear) (gravity)

If V_{g_i} and the friction factors were known, Eq. (12) would be suitable for predicting the void fraction in annular flow. The ways in which these variables are related to V_{f_s}, α, and ρ_f/ρ_g are not simple, however, and the equation is not useful for prediction. If Eq. (12) is made dimensionless the result is in terms of the parameters V_g^* and V_f^*, defined in Eqs. (3) and (4):

$$V_g^* = \frac{\alpha V_{g_i}}{\sqrt{\frac{\rho_f}{\rho_g}}\sqrt{gD}} + \sqrt{\frac{\alpha^{5/2}(1-\alpha)}{2 f_i}} \sqrt{1 + \frac{2 f_o}{(1-\alpha)^3} V_f^{*2}}. \qquad (13)$$

Let the interface velocity term be expressed as $\frac{K V_{f_s}}{\sqrt{\rho_f/\rho_g}}$, where

$$K = K(\alpha, \frac{\rho_f}{\rho_g}, V_f^*). \qquad (13\ a)$$

This is a way of saying that the interfacial velocity is a function of liquid velocity, void fraction, and density ratio. The liquid fraction is a measure of wall-film thickness, indicating a dependence of V_{g_i} on the distance the liquid penetrates into the gas space. Then density ratio is included as an indication that, for given V_{f_s} and void, large gas density will give larger interface velocity than will small gas density.

The form of the function K is unknown, but it is included as a multiplier of V_{f_s} for consistency with annular-flow experimental results. For very small liquid flows, the wall shear term in Eq. (13) is negligible; it can be seen in References (11), (12), and Figures 25 and 27 that lines of constant void fraction in annular flow start from $V_f^* = 0$ with positive, finite slope. For zero wall shear, the second term can make no contribution to the slope.

Putting (13 a) into (13) gives

$$V_g^* = \frac{K\, V_f^*}{\sqrt{\rho_f/\rho_g}} + \sqrt{\frac{\alpha^{5/2}\,(1-\alpha)}{2\, f_i}}\sqrt{1 + \frac{2\, f_o}{(1-\alpha)^3}\, V_f^{*2}}. \qquad (14)$$

(interfacial shear) (gravity) (wall shear)

The difficulties in using Eq. (14) to calculate the void in annular flow result from the facts that, even for a given pipe carrying given fluids,

$$\left.\begin{aligned} K &= K\,(\alpha,\, V_f^*), \\ \text{and} \qquad f_i &= f_i\,(\alpha,\, V_f^*), \\ f_o &= f_o\,(\alpha,\, V_f^*). \end{aligned}\right\} \qquad (14\text{ a})$$

On the transition line, however, there is a special relation between the void and V_f^*; fixing V_f^* fixes the transition void fraction. As the experiments show, the transition void is nearly the same for a three-to-one change in pipe diameter (Figure 24 a). Since the curves of void fraction vs. V_f^* are not in systematic order of diameter, and since the spread of the void in Figure 24a is only ± 2%, it can be said

that the transition void is a function only of V_f^* and not of pipe size. This is the criterion of transition for the annular flow model.

Then along the transition line, all the quantitites in Eq. (14a) are determined by V_f^* alone. In Eq. (14), specifying V_f^* then fixes V_g^{*+} if the relations of Eq. (14a) are known. These relations are not known, however, and the form of the transition line is available only from experiments.

It is possible, though, to show some qualitative results of Eq. (14) at the extremes of V_f^*. At zero liquid flow, the wall shear is virtually zero, and the transition line becomes

$$V_g^{*+} = \sqrt{\frac{\alpha^{5/2}(1-\alpha)}{2f_i}} . \qquad (15)$$

This result agrees with the experimental fact that a positive gas flow is required to hold up a wall film in a given pipe; the friction factor and void are fixed for a given pipe by V_f^*. But, as will be discussed in Chapter 4, there is a diameter effect which negates the statement that V_f^* alone is sufficient to specify f_i (though it is enough to fix the void).

If α varies but little along the transition line, Eq. (14) qualitatively predicts a concave-up relation between V_g^{*+} and V_f^*. The experimental transition lines are straight; this is partly due to the width of the transition band (Chapter 3) and perhaps also due to the complicated nature of the relations in Eq. (14a). As will be seen from the experimental data,

seen from the experimental data, there is no justification for more complicated presentation of the transition lines than straight lines.

At very high liquid velocities, the gravity term in Eq. (14) will become neglible compared with the wall shear and interfacial shear. Then Eq. (14) becomes, with the transition void fixed by V_f^*,

$$V_g^{*+} = \left[\frac{K}{\sqrt{\rho_f/\rho_g}} + \sqrt{\frac{f_o\, \alpha^{5/2}}{f_i (1-\alpha)^2}} \right] V_f^*. \qquad (16)$$

Again, if the void fraction varies very little along the transition line, as is the case for high liquid flow in the only experiment carried out in this region, the transition line becomes a line of constant flowing volume quality. Since the gravity term is neglected, and since the acceleration g appears in both sides of Eq. (16), it would be more appropriate to write (16) as

$$V_{g_s}^{+} = \left[K + \sqrt{\frac{\rho_f}{\rho_g}} \sqrt{\frac{f_o\, \alpha^{5/2}}{f_i (1-\alpha)^2}} \right] V_{f_s}.$$

2.4. Usefulness of the Analysis for Transition Studies

This annular-flow analysis, even with its highly oversimplified geometry, still contains the three undetermined functions of α and V_f^* listed in Eq. (14a). Even for annular flow, these functions would have to be found experimentally. For the special situation of transition the situation is even

worse; the unknown functions remain, and the physical mechanism of transition is still obscure. Thus the analysis can be used only as a dimensional analysis to suggest the appropriate dimensionless quantities for data presentation, and this is the only way it has been used.

As will be indicated in the discussion of the experiments, the analytical transition criterion (that the void is the same function of V_f^* for all pipe sizes) is appropriate, but the annular flow model still does not give the complete diameter effect. The transition value of V_g^* for the larger pipes at atmospheric pressure falls below the correlation; there is an unexplained diameter effect which requires further study. On the other hand, as the experiments will show, the V_g^*, V_f^* coordinates are quite effective over a range of diameters and densities which are of engineering interest.

2.5. Pressure Drop at Transition

If in Equations (7) and (8) the interfacial shear is eliminated, the pressure drop can be computed as

$$\left(-\frac{dp}{dz}\right) = \frac{2\tau_o}{r_o} + \rho_f \frac{g}{g_c}(1-\alpha), \tag{17}$$

or in terms of the definitions of f_o and V_f^*,

$$P \equiv \frac{\left(-\frac{dp}{dz}\right)}{\rho_f \frac{g}{g_c}} = 2f_o \frac{V_f^{*2}}{(1-\alpha)^2} + (1-\alpha). \tag{18}$$

Although this pressure-drop calculation should have application throughout the annular regime, Eq. (18) will be used only to report the experimental pressure-drop results along the transition line.

3. EXPERIMENTS

3.1. Desired Measurements

Although the bare minimum of desired results for a given pair of liquid in a given tube is the relation between gas flow rate and liquid flow rate for the transition line, it is evident that the void and pressure drop are of vital interest, and the connection among all four of these variables was the aim of the experiments. Although these four variables are of interest in their own right within a flow regime such as annular flow, it is also necessary, in an experiment intended to fix the transition, to add an indication of the existence or non-existence of annular flow. At the beginning of the study, too, it was not clear just which variables are important. In particular the influence of the surface tension and liquid viscosity were unknown, and it was determined to test their effects, especially since these two properties were excluded from the analysis.

3.2. Flow Apparatus

The flow system, which is sketched in Figure 4, consists of a vertical plexiglas tube about 20 ft. long supplied with gas and liquid through a mixing tee at the bottom. Having flowed together through the tube, the gas and liquid are separated in a baffled tank, after which the gas escapes to the room and the liquid drains into a weigh tank. In most of the tests the liquid was city water, which was discharged into the sewer after passing through the system. In the tests which

involved addition of other materials to the water, however, the mixture was returned to a reservoir and circulating pump after use in the test section.

Four static pressure taps are located at about five-foot intervals along the test tube; each tap is connected to one leg of a U-tube manometer, whose other leg is exposed to a controlled air pressure provided by admitting suitable amounts of high-pressure shop air into a manifold. Thus a variety of pressure levels in the test tube can be measured within the limits of length of the water-filled manometers. The static pressure measurements are used not only to obtain the pressure drop in the test tube but also to establish the pressure level at the regime-detection device; this latter measurement is needed to calculate the volume flow rate of gas at the detector.

Measurement of liquid flow is accomplished by timing the accumulation of liquid in the weight tank. The gas flow is measured by means of an A.S.M.E. square-edge orifice connected to suitable manometers of various ranges of sensitivity (0.1 in H_2O to 60 in Hg). The gas temperature is measured upstream of the orifice, and the liquid temperature is taken at the exit of the gas-liquid separator. This measurement gives a good estimate of the gas and liquid temperatures at the flow-regime probe without requiring a temperature sensor which protrudes into the test tube flow.

The void fraction is obtained by measuring the volume of liquid contained in the tube and subtracting it from the total

tube volume. Quick-acting valves are provided at top and bottom of the test tube; they are pneumatically moved together to isolate the test tube and divert the two-phase flow through a bypass tube which is identical to the test tube except that it contains no instrumentation. Use of the bypass tube almost eliminates back-pressure surges due to closing of the isolation valves; thus disturbance of the fluid supply and measuring apparatus is minimized.

Some additional details of the construction of the apparatus are given in an appendix.

3.3. Regime-Detection Probe

The device for determining the flow regime is a conductance probe virtually identical to the one built by Solomon[15] in 1962. A Chromel wire projects inward from the tube wall to the centerline, where it is bent downward for a length of about 1/4 inch. All but the last 1/16 inch of the wire's length is insulated with a thin tube of Teflon plastic, and the wire and Teflon sheath are supported inside a 1/16-inch O.D. stainless-steel tube as a cantilever from the tube wall. The assembly is sealed by a stainless-steel packing gland which permits adjusting the probe to center the exposed end in the tube. The probe, in place and removed from the tube, is shown in Figure 5.

A second Chromel wire is attached to the wall of the test tube opposite the probe and led out through the tube wall. The gap between probe and wall is in series with a 6-volt battery and a 2200-ohm resistor. An oscilloscope is connected

across the resistor as shown in Figure 6. The oscilloscope reads the voltage drop across the resistor, showing open circuit when no conducting liquid closes the gap between probe and wall and giving a recognizable signal when conducting liquid bridges the gap. An essential feature of this probe is the Teflon sheath, which water does not wet. The Teflon thus prevents a short circuit from a drop of water which may cling to the exposed end of wire, completing a circuit along the sheath and around an annular water film to the wall wire. The drying time of the Teflon tube after passage of a plug of liquid is extremely short, less than 10^{-3} seconds as observed with the oscilloscope.

3.4. Interpretation of Probe Output

The purpose of the probe is to show the presence of liquid which bridges from the tube centerline to the wall. The extent to which it does this correctly is dependent finally upon visual observations of flows whose liquid velocities are low enough to permit direct study by eye. Thus the use of the probe for higher-speed flows, where the geometry is unavailable by direct visual observation since the appearance of the flow field is only a blur to the unaided eye, requires the assumption that the probe indications at high speed have the same meaning as at low speed. A valid means of checking this assumption is to increase the speeds available to visual observation through use of high-speed motion pictures. Such pictures were taken for a few flows, both low-speed and high-speed, for which the probe indication was interpreted to be

either annular or semiannular. The probe indications for annular and semiannular flows were consistent between high speed and low speed in that the picutures of flows which the probe said were semiannular displayed slugs of liquid bridging the entire tube, while the flows with annular indications showed no bridges. It is thus concluded that the use of the probe at high flow rates is appropriate, and the oscilloscope display of the probe output is taken as the fundamental indicator of flow regime.

Before presentation of descriptions of the various probe indications for flow regime, it is desirable to restate the nature of the transition being sought, i.e., the transition criterion being applied. The criterion is the occurrence of slugs of liquid which fill the tube. If such slugs do not occur, the flow is said to be annular. If such slugs do occur, the flow is said to be semiannular. This is the geometric definition of transition. Operationally, it represents a change in the mode of liquid transport, from a rough-surface annulus in which liquid flows as it is sheared in the bulk of the annulus or by the motion of surface waves, to a series of slugs which bridge the tube and carry a substantial part of the total liquid flow. As a check on the quantity of liquid carried by the slugs, spot checks were carried out during a number of the regular tests in the following way: The number of slugs passing the probe was counted over an interval of time. The length of each slug was estimated by noting the

(average) time required for passage of a single slug by scaling on the oscilloscope screen and multiplying by the slug velocity, which was assumed to be the same as the superficial gas velocity. The liquid volume flow rate due to the slugs was then compared with the total liquid volume flow rate and was found (with consistency commensurage with the rather rough precision of measurements) to be about 10% of the total for flows judged to be "high semiannular" and about 20 - to 25% for flows called "definitely semiannular." It is thus concluded that the geometric criterion of transition has physical meaning in terms of a change in the mode of liquid transport.

The oscilloscope displays typifying the various flow regimes, along with the terms used to classify the transition flows, will now be described. If the flow is annular, far from transition, there is an open-circuit indication on the oscilloscope screen, and one observes no departures from the zero-signal trace over a long time period, say, several minutes to an hour. In the data presentation, this flow is called "definitely annular," or for short, "annular." As will be indicated later, annular flow without entrainment is not the only flow regime which could exist with this probe indication; the probe system is not capable of detecting spray particles in the gas core. But if the spray regime is included with annular flow on the basis that the gas is the continuous phase and the possibility of confusion is kept in mind, the probe output is useful.

If, upon progressive reduction of the gas flow rate, there appear on the screen occasional small, single "pips" of brief duration, the flow is considered still to be annular but to be showing the first signs of oncoming transition. This flow is referred to as "low-annular," and in the context of the tests it is at or near the lowest gas flow which will support an annulus of liquid at the preset liquid flow rate. The small single pips are interpreted as single large waves which reach the centerline but do not necessarily bridge the entire pipe.

Further reduction of the gas flow increases the frequency of the pips, and the pips begin to appear in groups. When the groups become well-defined steps in the oscilloscope signal which represent plugs of length ranging from a few inches to a foot (assuming they move at throughput velocity), and the steps arrive fairly regularly at intervals of a second or two, the flow is said to be "high semiannular." This is the flow which delivers about 10% of the liquid via the slugs. The remainder is transported either as a climbing annular film or as spray. Photographs of the oscilloscope trace during passage of a slug are shown in Figure 7. The alpine appearance of the slug is interpreted as bubbles in the slug. The traces are of irregular shape, but they usually are preceded and followed by waves which do not quite bridge, as indicated by the "growth" of the step at its beginning and end. Once the main part of the slug has arrived, however,

the signal is flat except for the sharp valleys representing the small bubbles.

A slight further decrease of gas flow causes the steps to arrive more frequently (one or two per second), and the flow is said to be "definitely semiannular," or "semiannular" for short. Figure 7 is as valid a picture of "definitely semiannular" flow as it is of "high semiannular," and this brings up the point that a single still photograph of either the flow itself or the oscilloscope trace is inadequate to define the flow regime. The flow between slugs is in every respect an annular flow, and unless some means is provided for the slugs themselves to trip the camera, still photography is likely to convince the observer that annular flow exists unless he is lucky enough to snap the shutter at just the right instant. For a permanent record which would determine the flow regime, moving pictures would be needed. The oscilloscope gives no permanent record, but while the experiment is going on it gives the observer the same kind of information he could get from moving pictures (and could not get from still pictures or other single-shot indicators). This notion received emphasis at the time the pictures for Figure 7 were made. The cathode-ray trace clearly indicated semiannular flow, but a dozen or more trials were required to capture a single slug trace.

It could be argued that movies would be a satisfactory direct means of noting the flow regime without recourse to a detector probe and oscilloscope pattern which requires

interpretation. But it is just the impermanence of the oscilloscope trace which renders it convenient for these kinds of tests; many miles of film would be required for direct observation of the same phenomena displayed by the oscilloscope at zero cost of materials.

As a matter of incidental interest in connection with the meaning of the probe signal, it should be mentioned that the device gives recognizable patterns for stable slug flow and bubbly flow. The plugs of stable slug flow are identifiable by their regularity and by the fact that they are not preceded by waves which cause the signal to build up upon arrival of the plug; the rise of the 'scope trace is sharp, and it reaches the full-scale value almost instantaneously. The presence or absence of bubbles in the plug is indicated in the same way as for semiannular flow. Bubbly flow is also identifiable by the fact that the 'scope trace shows the "all water" indication, modified by the sharp-pointed "valleys" which show the bubbles. A number of displays of the various flow regimes as obtained with a Sanborn recorder are given in reference (15); again, the Sanborn gives a permanent record, but the faster response and convenience of the oscilloscope make it a better choice for present purposes.

There arises the question of the possibility of spurious indications from the flow regime probe. Reference has been made to spray and the inability of the probe to detect spray. As will be mentioned in the discussion of experimental results,

through, some of the effects which appeared in the experiments are attributed to the presence of spray. In particular, the transition line was found to move to higher gas velocity in a region where spray is believed to occur, and the question arises: Can a cloud of spray droplets give a spurious indication that a slug of liquid is passing the probe?

The notion is that a dense cloud of spray droplets might supply so much water to the probe and its Teflon shield that the Teflon would not have time to dry between droplet arrivals, and a short circuit would occur along the shield. It is not clear that the spray does arrive in dense clouds, but even if it does, the probe should succeed in drying rapidly enough to avoid the erroneous reading. It is capable of showing the presence of a bubble which is 0.1 inch long and moving at, say, 50 fps. This requires that the probe dry in less than 2.10^{-4} sec. In addition, the short circuit would give a reduced amplitude of signal, since the film of water on the Teflon shield must have very small cross-section for conduction as compared with a bridging wave. No such effect is observed, and one concludes that the slug patterns observed in transitions at high liquid flows are genuine.

Several other effects can be observed in connection with the regime probe. The fluid used most often in the tests was tap water; addition of an organic material, specifically glycerine, caused a depression of the oscilloscope signal due to the lowered conductivity of the fluid. Increasing the pipe diameter also reduced the amplitude of the trace. Also, when

water was the working fluid, if the test tube was filled with stationary water, a large signal was obtained. If the water was then caused to flow, the signal decreased, and it continued to decrease as the water velocity increased, levelling off gradually so that at a water velocity of about 5 fps there seemed to be no further decrease. It is speculated that this is an "electro-kinetic" effect, associated with the charge-carrying capacity of the water.

If the amplitude of the signal were important to the results, this effect could have been dangerous, but the amplitude was not stressed in the tests. The consistent indicator was the appearance of wave signals in long groups, indicating the presence of bubbly slugs. The oscilloscope trace was not used quantitatively, except in the spot checks to estimate the slug length, and this estimate made use of the time scale, not the amplitude.

3.5. Conducting the Tests

Experiments were conducted to determine the effects of liquid flow rate, tube diameter, gas density, surface tension, and liquid viscosity on the minimum gas flow rate which could support annular flow. The broadest range of superficial velocities was obtained for the smallest (1/2" I.D.) of the three pipes tested, because of limitations on the rates of air and water flow which could be supplied steadily and continuously. The procedure for the 1/2" pipe is typical of all three.

With the choice of liquid and gas made for the chosen

pipe, the remaining independent variable is liquid flow rate. The tests were conducted in series of approximately constant Q_f by setting the liquid-flow control valve at the start and varying the gas flow; Q_f was only approximately constant because no changes were made in the valve setting. As Q_g was reduced the Q_f usually increased slightly due to the reduction of back pressure at the mixing tee. In each series the first data point was chosen to be well into the annular region (as indicated by the probe), and successive tests were made with gradual reduction of Q_g. At each data point the necessary data to obtain Q_f and Q_g were recorded, manometer readings were recorded to give pressure gradient and pressure level at the probe location, and the oscilloscope's flow regime indication was noted. For many, but not all, of the points, the quick-acting valves were used to isolate the test pipe, and the liquid fraction was noted. Successive reduction of gas flow caused successively closer approach to semiannular flow, and data points were recorded in each series to give at least one point in each of the "definitely annular," "low annular," "high semiannular," and "definitely semiannular" categories.

Not all the data points were taken close to the transition line. Since the apparatus is well suited to measurements in both the annular and semiannular regimes, tests were made at various water flows to give pressure drop and void fraction at air-flow rates which were well removed from the transition line in both directions. The purpose of this work was to make

available some controlled-experiment data in these regimes to provide an anchor for future studies of the non-transition properties of the two regimes, as well as to give a more complete picture of the two regimes which are divided by the transition lines whose study is the object of the present research.

After reduction of the flow-rate data, the points were plotted one by one on a work sheet which was in the form of a flow map of V_{g_s} vs. V_{f_s}, each point being labelled according to its flow regime, such as "annular," "low annular," etc. Completion of a number of series of tests permits one to see on the flow map a region which divides all the "semi-annular" points from the "annular" points. The centerline of this region, estimated by eye, is used to denote a single transition or dividing line between the two regimes. The data for the 1/2" pipe, with air and water flowing, are shown along with the transition line interppretation in Figure 8. The numbers near the data points indicate the measured void fraction.

To study the effect of changing the liquid properties, additions were made to the water. The liquid viscosity was roughly doubled by addition of 25 volume per cent of glycerine. The liquid density also varied slightly, increasing by 5% over that of the tap water. The recirculating pump and reservoir system for the mixed liquids was substantially less reliable than the city water supply, and the data taken with other materials added to the water were consequently much abbreviated.

But several series of tests showing the transition line vs. liquid throughput were made, and the effect of doubling the viscosity on the transition location was found to be small, well within the limits of precision to which the flow regime itself is known.

Similar tests were made with the addition of 2 1/2% methyl alcohol by volume. A difficulty arose when it became apparent that the air flow was stripping the volatile methyl alcohol from the solution, with the result that, after an hour or so of running, the alcohol content of the water was much reduced. This problem was overcome by turning to the less-volatile ethyl alcohol, operating only long enough to get one data point, sampling the solution for later surface-tension measurements, and discarding and replacing the entire solution after obtaining a pair of data points which bracketed the transition line. The surface-tension measurements later showed that the loss of alcohol under these conditions was negligible, the surface tension varying less than 1/2% from a nominal value of about 57 dynes/cm. The influence of the surface tension reduction was negligible in the low-liquid-flow region. The density variation due to the addition of alcohol was very small.

The gas density was altered by substituting carbon dioxide for air. Three tanks of CO_2 at 1000 psi were manifolded together, and after suitable reduction of pressure the gas was admitted to the system in the same way as the air was. It was necessary to pass the CO_2 through a coil of copper tubing

immersed in water to avoid excessively low gas temperatures due to expansion. Long-term operation was not feasible, but 18 data points were obtained which gave a good indication of the transition location. It was necessary to make a correction on the gas velocity for the solubility of CO_2 in water; a volume of water will dissolve about a volume of CO_2 at atmospheric pressure, and it was assumed that the solution was saturated before it reached the flow-regime probe. Substitution of CO_2 augments the gas density by about 53% over the density of air; the result was a lowering of the transition gas velocity.

The limit of liquid superficial velocity for which the air supply was sufficient to provide annular flow in the 1/2" tube was about 2.7 ft./sec.

Similar tests were made with two other pipes, 1" and 1.5" - I.D. In the 1" pipe virtually all the data were obtained with air and city water. Two check series were obtained with glycerine added, and little or no effect on the transition line was found. A single pair of check points was run with 2 1/2% methyl alcohol, with no apparent effect on the transition. In the 1-1/2" pipe, the only fluids used were air and water. The maximum water velocities for which annular flow could be sustained in the 1" and 1.5" pipes were about 1.4 and 1.2 fps, respectively.

The low transition gas velocities found for the 1.5" I.D. tube raised the question whether the form of inlet might influence the transition line location. The inlet was changed

from a simple tee (Appendix C and Figure 32) to a mixer in which the liquid is admitted through a series of small holes in the tube wall and the gas enters from the bottom through an entrance which is concentric with the tube.

The appearance of the flow was altered near the inlet, but a few feet above the inlet the flow was the same, visually, as with the mixing tee. There was no significant effect on the transition line, as shown in Figure 13a. This indicates that the differences between the large and small pipes were a result of pipe size and not entrance conditions.

3.6. Precision of the Measurements

The most repeatable and most readily checked of the measurements are the gas and liquid flow rates. The carefully made A.S.M.E. orifices are said by Leary and Tsai[16] to give results within 1/2% if the appropriate corrections are made. Since the data were reduced by slide rule, the processing introduces errors of 1/2% or more, but the overall errors on gas velocity should hardly exceed 1%. The liquid-flow measurements are at least as precise, since they were made by a calibrated platform scale and an accurate stopwatch. The flow was averaged over several minutes, during which the accumulation of liquid ranged from about five pounds to 80 pounds. The greatest errors are at the smalllest liquid flows where it was not convenient to wait for accumulation of large amounts of liquid. Comparison of the scale indication for samples as small as 5 lb. between the platform scale and an accurate balance, however, showed no measurable differences between the

two standards. An independent check on the liquid and gas flow measurements was made possible by comparison with Wallis's data of August, 1963[17]; both Wallis and the author had made annular flow void measurements in a 1" pipe, and when plotted together on a flow map the results were virtually indistinguishable, one from the other. A further confirmation of the air-flow results was obtained when the pressure drop in the 1/2" tube, operated dry, was measured and used to compute the air-flow (independently of the orifice pressure drop) via a friction factor obtained from a Moody chart. The agreement between this method and the orifice method was perfectly satisfactory, being well within the accuracy one normally expects in figuring the friction factor.

The void and pressure-drop results, on the other hand, are more in doubt. For flows which were definitely annular, there was little difficulty in repeating measurements of these parameters. But as the annular flow was made more nearly semi-annular, fluctuations began to appear within a given test. The pressure level at each pressure tap, as indicated by position of the manometer free surface, could vary as much as $\pm$ 0.3 in Hg, or about $\pm$ 10% of the local gage pressure. Figured as a fraction of the pressure gradient between taps, this error would result in a pressure-gradient error of as much as 12.5% in a typical case, if the extremes of the manometer swings were used instead of the average. An attempt to minimize such errors was made by provision of small valves to damp the fluctuations and by estimating the midpoints of the manometer excursions

when recording the data. That the pressure surges are real is not in doubt; the large waves in low annular flow and the slugs in semiannular flow represent concentrations of pressure drop, and the passage of one of these concentrations past a tap causes the fluctuations in manometer readings. Since there are no other data precise enough to indicate how seriously the averaged pressure figures may be in error, the only recourse is to rely on the internal consistency and repeatability of the measurements within the present experiments.

A somewhat similar situation prevails for the void measurement. Near the regime boundary, and for semiannular flow in general, the liquid holdup measured by use of the quick-acting valves is a function of the number of slugs of liquid (or large waves) caught in the tube during the measurement. Since this number varies in irregular fashion, the measured liquid holdup varies in a given test. It is thus necessary to isolate the test tube several times for each void measurement, repeating the measurement enough times to give a hopefully representative sample. To indicate which value within a given spread should be used and whether enough trials had been made, a simple, intuitively based method was used. When the average of all readings was roughly the same as the median of all readings, the average figure was said to represent the void fraction for the present flow conditions. No attempt was made to apply any sort of sophisticated statistical method, as the calculations had to be made in the

laboratory while the tests were in progress; also, the time required for the void measurements far exceeded that needed for all other parts of the tests, so the number of trials for a correct void figure in a given test was practically limited to five or six.

In the region of the annular-semiannular transition, the deviation of extreme values from the mean was at most about $\pm$ 2 1/2% of the liquid fraction. Since the void was about 80%, this extreme error would be only about $\pm$ 0.6% of the void fraction. The deviations generally tend to increase as one goes farther into semiannular flow, and for several runs in the 1 1/2" pipe at about 50% void (slug flow), the spread was $\pm$ 4% on both liquid and gas fraction (that is, $\pm$ 4% of 50% = $\pm$ .02 spread on the absolute void value).

Even though the flow-regime probe was not used in a quantitative way, the question of precision arises in connection with its use. The geometric transition criterion is still arbitrary, and the means of identifying the flow regime is still a visual one. It is a much more satisfactory means, however, than direct observation of the flow through a transparent tube wall, especially at high flow rates. Still, the pattern requires interpretation, and the lack of sharpness in the transition boundary is reflected in the spacing between data points labelled "low annular" and "high semiannular." This spacing is surprisingly constant, and it gives an indication of the precision of the probe reading in terms of gas velocity. In the 1/2" pipe this spacing is about 20 fps of

gas velocity. The fractional deviation becomes quite large for the lowest transition gas velocities; at zero liquid flow when the transition gas velocity is about 30 fps (expressed now as a single value) the fractional spread is ± 33%. At the highest liquid rates this figure drops to ± 10%. The point is that the transition line is far less precisely located than the flows, pressure drop, and void are measured, and no improvement in the precision of these latter figures will increase the certainty with which the transition velocity is known.

3.7. Direct Presentation of Data

The results are presented in the form of flow maps (V_{g_s} vs. V_{f_s}) for each of the conditions tested. To facilitate interpretation of the raw data by the reader, the individual data points are shown with the flow regime indicated, and the single line intended to show the transition compactly is drawn as a best fit to the dividing region between the two regimes. Figures 8 through 13 and 13 a give these data, and the individual test point results are tabulated in Appendix A.

In the Summer of 1963, Griffith[18] measured gas and liquid flows for the annular-semiannular transition in steam-water flow through vertical pipes. He used the same flow-regime probe and transition criterion as in the presently reported experiments to locate the transition in a five-foot-long unheated section supplied with steam and water from a heated section upstream. Although he did not measure void and pressure drop, he obtained annular and semiannular data

for three pipe sizes (.375", .625", and .875" I.D.), at three pressure levels (200, 400, and 600 psig) for each diameter. Thus his tube diameters are in the range tested with air and water, but his higher pressure raises the ratio of gas density to liquid density. Figures 14 through 22 show Griffith's individual data points with the present authors interpretation of the correct single-line representation of the transition. Appendix B lists the numerical data.

In each of Griffith's experiments the transition line became a line of constant quality (Q_g/Q_f) for the higher values of liquid flow, and the transition line drawn in Figures 14 through 22 is such a line. It is not possible, however, to separate the annular and semiannular points at low liquid flow by a constant-quality line. This effect is most noticeable in the 0.875" pipe, less clear in the 0.625" pipe, and not noticeable at all in the 0.375" pipe. In the two larger pipes it is necessary to bend the transition line toward the V_{g_s} axis at low liquid throughputs to give reasonable separation of the points representing the two regimes. Thus there are two parts of the transition line in Griffith's data, as well as in the low-pressure, air-water results illustrated in Figures 8, 9, and 10. The nature of the transition differes between the two parts of the curve, and comments on the difference will be made in Chapter 4.

It is not possible to draw the transition line for low liquid flow for all of the steam-water data. Griffith had a great deal of difficulty in controlling and measuring the

liquid velocity at low flow rates; thus low gas velocities are not reported for his..375" tube, and the low-flow region does not appear. In the .625" tube there are enough data to suggest a bend in the line, but not enough to fix it firmly. But the 0.875" tube clearly shows the effect at all pressures. These data are as well correlated by Equation (15) as later modified in Chapter 4 as are the air-water data.

The shape of the transition line on a flow map of superficial velocities is thus reported as a straight line for low liquid flows and a straight line through the origin if the liquid flow is sufficiently high. A quantitative discussion of the bent line will be given in Chapter 4.

The void fraction and pressure drop along the transition line are plotted in Figure 24 for the air-water two-phase flows. For the 0.5" pipe there are breaks in these curves at the same value of liquid flow as that which produces the jump in transition gas velocities. In the 1.0" and 1.5" pipes, the flow was not large enough to produce a jump. The important point in connection with the transition void is that it varies rather little, being always less than 90% and more than 80%, and it is the same function of V_f^* in all three pipes.

The numbers used to plot the curves in Figures 8, 12, 13, and 24 are tabulated in Appendix D.

Enough void and pressure-drop measurements were made with air and water in the annular and semiannular regimes to

permit presenting results for these variables. This is done by showing lines of constant void fraction and pressure drop on flow maps, as in Figures 25 through 27. This method of plotting the results involves interpolation from data point to data point, with the need to interpret any local mismatches among the interpolated values, but it has the advantage of presenting all the data for a single pipe on a single page. The lines of constant void fraction are seen to be straight for annular flow. They tend to become concave down for high liquid flows above the transition line; this effect is interpreted by Wallis[12] to be the result of spray. In semiannular flow the lines of constant void fraction are concave down.

The lines of constant pressure drop show both positive and negative slope, and they are concave either to the left, as for the lowest pressure drops, or to the right, as for the highest drops. No attempt is made to correlate or interpret these data; they are presented as incidental to the main work. These curves, being the results of interpolations, should not be used to replot the void and pressure drop as ordinates. Appendix A gives the raw data which may be used for that purpose.

4. CORRELATION AND INTERPRETATION OF EXPERIMENTAL RESULTS

4.1. Transition Gas Velocity

Equations (14) and (14a), along with the dependence of transition fraction on V_f^* along the transition line shown in Figure 24a, suggest that the flow maps be presented on coordinates of V_g^* vs. V_f^*. The transition lines for the 0.5" pipe, air-water, and the 0.875" pipe, steam-water, fit the equation

$$V_g^{*+} = 0.9 + 0.6\ V_f^* \qquad (19)$$

virtually perfectly up to the point of the jump or break-point in the transition line, as shown in Figure 28. The smaller pipes with steam-water are not included, because no firm data are available. The air-water results in the 1.0" and 1.5" pipes fall below the correlation, the depression being greater for the 1.5" pipe. The poor correlation for these two tubes is discussed in Section 4.3.

The agreement between the 0.5" air-water and 0.875" steam-water results is so close that quantitative comparisons are inappropriate; the differences between the transition lines for the two tubes are small compared with the breadth of the transition band. That is, the agreement between the correlated lines is better by far than the precision of the definition which locates the lines.

The bulk of the data show the break point in the transition line to be in the neighborhood of $V_f^* = 1.0$. This figure is hardly precise, but it does fairly represent the break point for most of the data. The anomaly of the CO_2 - water curve

is not explained; it fits the correlation perfectly but continues to $V_f^* = 2.4$ before reaching the break point. The validity of this result is somewhat in doubt due to a paucity of test data. If one ignores this single anomaly, though, it appears reasonable to state the range of validity of Eq. (19) as

$$V_f^* \leq 1.0. \tag{20}$$

The region in which Eq. (19) is applied is interpreted as that in which the transition occurs from annular flow (without spray) to semiannular. This is the region in which Wallis (11) was working when he used his counterflow flooding results to predict the zero-liquid-flow transition point. He obtained values of V_g^{*+} ranging from 0.8 to 0.9 for $V_f^* = 0$, and this agrees with Eq. (19). Wallis's latest results (12) call for a lower value of V_g^{*+} at the starting point, but his criterion of transition has changed, and he is looking for a direct transition to sloug flow. If one were to plot the intersections of lines of constant void fraction calculated for annular flow from Reference (12) with slug flow lines of constant void from Eq. (1) there would result two loci on the flow map, one at about 70% and one at about 80% void (for a 1" pipe and air-water), which qualitatively demarcate the slug, semiannular, and annular regimes. Temptation to use this approach is avoided here in view of the fact that the measured voids for the "geometric" transition criterion exceed the voids which are possible in slug flow for the liquid flow rates involved. Many of the measured voids are in the neighborhood

of 85%. Equation (1) does not permit any upflow of liquid for voids over 83.3%, and voids in the neighborhood of 81% or higher require huge gas flows to sustain small liquid flows. Idealized theoretical models of well established regimes are in fact not likely to succeed at or near flow regime boundaries, where the relative importance of the various forces is changing. It appears quite inappropriate, then, to seek a direct intersection of slug-flow theory with an annular-flow correlation, and there is no reason to expect such an itnersection to predict the change in geometry. The nature of the change of geometry and the fact that a slug-flow solution is not possible both lead to a comparison with the zero-liquid-flow results of Reference (11) as a realistic view of the work of others.

Although the present flow model contains no suggestion as to the physical mechanism of transition, the flooding mechanism is attractive. The flooding line of Reference (10) is for counterflow, not cocurrent flow, but it was observed in the present experiments that downflow of the liquid often occurred in annular flow before and after the passage of a large surface wave. At least at the low liquid flow rates the conditions for flooding are temporarily present from time to time at every location in the pipe; under these conditions the pipe locally becomes a countercurrent column. The difficulty is again the temporal nature of the flow due to the interfacial waves. So far it has not been possible to describe the counterflow region sufficiently well to permit an analysis

which would include the flooding effect in a quantitative way.

Beyond the break point in the transition line, a jump and change in slope, or merely a change in slope, to a constant-quality line, indicates a change in the nature of the transition. The flow-regime probe shows no noticeable difference between the low-liquid-flow and high-liquid-flow regions on the semiannular side of the transition line. It is incapable of detecting spray in the gas core; thus other means must be resorted to to justify the conclusion that the change in transtion line shape is the result of spray. There is a suggestion of this change in Reference (12). In his entrainment studies, Wallis defines the onset of spray liquid transport by extrapolating the entrainment flow rates to zero entrainment. In a 0.975" -diameter tube using air and water, he found the dimensionless gas velocity for zero spray to be $V_g^* = 1.45$. If his curves are extended in the other direction to 100% entrainment, the resulting V_g^* is 3.07. The corresponding values of superficial gas velocity in a 0.5" -diameter tube would be 48.4 fps and 102.5 fps for zero and 100% spray. These match very closely with the break points on the 1/2", air-water transition curve, as the jump begins at 54 fps and ends at 90 fps. The close match is perhaps fortuitous. The possible Weber Number criterion, Equation (6), predicts a <u>rise</u> in the critical gas velocity with reduced diameter, but Wallis has not been using this standard in his more recent work, and he has been putting emphasis on the critical value of V_g^*, though he states (12) that this is not likely to be sufficient to specify spray flow completely.

The means by which the presence of spray promotes the transition to semiannular flow is not clear. It may be speculated that the production of spray droplets will be greatest in the vicinity of the largest interfacial waves, where the gas velocity is greatest due to reduced area and the shear strain rate is augmented. This would produce clouds of spray particles which would be denser than the average, and one of these clouds might contain sufficient liquid to cause bridging upon catching up with another large wave. If the droplets move at nearly gas velocity, they would indeed overtake the surface waves. Whatever the pre-transition geometry and dynamics may be, the means by which the presence of spray promotes transition deserves further study.

In the course of the experiments there was some question at first as to whether this effect was a real one as opposed to some peculiarity of the experiment itself. The jump was observed only in the 0.5-inch pipe, but it was observed with all the materials used. Repetition of the tests, and stiffening the tube support structure to eliminate possible deflections of the rather flimsy tube, served only to cement the notion that the effect is a real one. Then, the data of Reference (18) showed similar breaks and change of slope to the constant quality line, and the jump was confirmed as an experimental fact. The break points, which are very widely separated in the raw data, are fairly well brought together when the V_g^* and V_f^* coordinates are used. If the

extremes are ignored, it could be said that the breaks occur at values of V_f^* from about 1.0 to 1.5 and values of V_g^* from about 1.5 to 2.0.

The constant-quality transition line at high liquid flow can be examined by use of Eq. (16a). The void fraction at high liquid flow in the 0.5" pipe changes very little along the transition line. Since the transition-line slope is constant, it appears that the remaining terms of Eq. (16a) are also constant or nearly so. Changing density ratio, however, has a large effect on the slope of the transition line, as shown in Figure 23. Equation (16a), with its two terms in the brackets, suggests that the simple 0.5 power on the density ratio is not sufficient to correlate the high-liquid flow transition, and this is illustrated in Figure 29. As can be seen in the same figure, the diameter effect is weak, but the density effect is strong. If the data are used to establish an expression, strictly empirically, the result is

$$V_{g_s}^{+} = \left(7 + .06 \frac{\rho_f}{\rho_g}\right) V_{f_s} \qquad (V_f^* \gtrsim 1.5). \tag{21}$$

This expression fits the data to within $\pm$ 20% at worst for the high liquid throughput region. Although Eq. (21) compares favorably with Eq. (16a), the means by which the exponent on the density ratio is fixed is not clear, and the details of the spray-slug transition are left to future research. Figure 29a shows the comparison of Eq. (21) with the data.

5.2. Transition Void Fraction

The void at transition is seen to decrease from just under 90% at zero liquid flow to minimum values of 81-to 86% for the three tubes tested. In the 1" tube the measured transition void levels off at about 86% at the highest liquid velocity, and in the 0.5" tube the lowest value of about 81% is suddenly raised to about 86% by the spray jump, and it fairs into a line of 87-to 88% void for further increases in liquid flow. Characterizing the void by a single number in this region is analogous to writing a single figure for the interfacial velocity; neither is correct in that both vary widely and irregularly in both time and position. In the tests the average void for the entire 20-foot length of tube was used to represent the void at the flow-regime probe, and one would expect the void to increase somewhat as the flow proceeds downstream, due to expansion of the gas. But the intent of the experiment was to represent pipes of common size and length, and it was judged to be just as appropriate to measure the void over the entire length as to use only some shorter length at an arbitrary location in the tube with no rational basis for choosing that location. Neither procedure can give the true, time-varying local void. These are serious limitations on the precision of any holdup-void measurements, and a statement about transition void fraction should admit its own inaccuracy by avoiding too-precise reporting of a badly measured quantity. A statement which fits these limitations is the following: If the average void frac-

tion exceeds 90%, the flow will be annular, and if it is less than 80%, the flow will not be annular.

The equivalence of transition void among the three pipe sizes has been discussed in Chapter 2 and is illustrated in Figure 24a.

4.3. Testing the Flow-Model Assumptions

In the experiments the assumption of steady and one-dimensional gas flow for annular flow was reasonably well met, at least in the average. At the highest flow rates for the two phases there was in fact some surging due to the violence of pressure fluctuations near the transition line, but for well established annular flow the gas flow was steady. The liquid flow was never steady, and the characterization of the liquid flow by a single interface velocity is admittedly unrealistic. The only justification is an acceptable correlation with the parameters suggested by the model.

The assumption that the gas density is constant along the length of the control volume analyzed was accounted for in part by evaluating the gas density at the flow regime probe from pressure measurements. At very high pressures, where the pressure drop is small compared with the inlet pressure, the assumption is fully justified; in long, low-pressure systems it would be less satisfactory. But errors due to use of an average density would be worst at the highest gas and liquid flow rates and least at zero liquid flow, where the gravity term should control the pressure drop. Since the experiments show the (dimensionless) pressure drop at this

condition to be just the weight of the liquid column supported, it is concluded that the effect of gas expansion in the region where the correlation is applied is satisfactorily accounted for by using the gas density at the probe. In the analysis, the expansion effect was masked in the unknown form of the interfacial velocity, which was never computed. Even if it had been, the effect would have produced just another density-ratio dependence, with no effect on the choice of correlating groups.

The assumption that the viscosities will not be important was checked directly by the experiments with glycerine and water. There was no influence on the transition-line location, for either low or high liquid flow, although the jump in the transition line moves to a new location. It is concluded that omission of liquid viscosity from the model is appropriate.

Likewise, changing the surface tension has no effect on the low-liquid-flow transition. The jump location changes, however, and the constant-quality line for high liquid flow differs from that for air and water (compare Curves laand 2 in Figure 23). The influence of surface tension should be most apparent in the smallest tubes; the 0.5" tube is large enough to avoid the effect.

4.4. Pressure Drop Along the Transition Line

If the transition pressure drops of Figure 24 are replotted in dimensionless form according to the definition of

Eq. (18), the results are as shown in Figure 30. At V_f^* = 0, at which $\tau_o \doteq 0$, Eq. (17) predicts that P^+ is just the liquid fraction, which is confirmed by the experiments. The measured liquid fractions for the 0.5", 1.0", and 1.5" pipes at zero liquid flow are 0.13, 0.11, and 0.14 in the same order, and for all three pipes the measured P^+ is .125. Therefore $P^+ \doteq (1 - \alpha)$ to within $\pm$ 12% at zero liquid flow.

Although no attempt has been made to correlate the transition pressure drop, it would be desirable to compare Eq. (18) with the measured P^+. In an attempt to see whether the entire P^+ curve for the 0.5" pipe could be represented by Eq. (18), an arbitrary point on the experimental curve was chosen, namely, $V_f^* = 2.0$, for which $P^+ = 3.16$ and $\alpha^+ = .870$. For this point, Eq. (18) gave $f_o = .00640$. The friction factor was then taken to be proportional to the actual (not superficial) velocity to the 0.2 power, and Eq. (18) was used to predict P^+ for the entire curve, using the measured void at all velocities. The result is plotted in dashes on Figure 30; it fits the data for all three pipes within $\pm$ 20% at worst, even in the low-liquid-throughput region. The fitting-point was deliberately chosen in the spray-transition region, but Eq. (18) successfully predicts the transition pressure drop in both regions, all the way to zero liquid flow. This suggests that the liquid behaves in a turbulent fashion along the transition line, even to the lowest liquid flows. It may be possible to correlate pressure drop for the annular flow regime in a similar way; at least this close fit at the

transition is encouraging. For comparison, the method of Lockhart and Martinelli[1] was used to compute the pressure drop along the transition line, using the measured values of gas and liquid velocities for the 0.5" pipe. The results fall below the experimental data, being about 30% low at the end of the low-throughput region and about 50% low at the highest liquid velocity tested. The curve-fit does better over most of the range, except at the lowest liquid flow, but this method requires an experiment. Present methods (Martinelli) will predict the transition pressure drop within a factor of 2 without using an experiment, and this is the level of prediction which remains to be improved upon.

4.5. Extension of Results to Other, Untested Conditions

Although emphasis has been placed on the effect of pipe diameter, the acceleration of gravity appears with the diameter, and alterations of g would have the same effect as the diameter. Reducing g would lower the velocity required for transition at zero liquid flow, but the slope of the transition line would remain the same. Zero g would cause the transition line to be a constant-quality line. Changing g would have no effect on the high-throughput data, as indicated by Eq. (21).

If the pipe is made horizontal, there should be no effect on transition for high liquid throughputs where the shear stress dominates. No prediction is made for horizontal tubes in the low-liquid-flow region, however, since the flow cannot be one-dimensional as was assumed in designing the model.

Similar comments apply for intermediate angles; if the flow is large enough so that gravity (in this case, its direction) is unimportant, then the transition will be independent of the tube angle.

If the geometry is different form that of a circular tube, an equivalent diameter based on volume and wetted area is recommended as a substitute for D. This is by analogy with the procedure used in dealing with heat exchanger surfaces and other complicated geometries; the gas-liquid interface should be equally chaotic in any geometry, and the driving shear stress should have about the same role as in the round tube. A test of this idea was made "in reverse" in Reference (10), where Wallis used the equivalent diameter in packed beds to correlate flooding, and then chose the tube diameter as the analogous dimension in pipes.

Although the data involving viscosity are not numerous, and although they were in fact used to indicate that viscosity has little or no effect, the pressure drop Equation (18), along with the remarks on the transition-line pressure drop, suggests that the wall friction factor will increase as $\mu^{0.2}$. This will increase the pressure drop required to drive a given liquid flow rate in annular flow, requiring a greater gas velocity at a given void. This notion is based on very thin evidence, but if the liquid viscosity varies greatly from that of water, to the point where the 0.2 power may be significant, the method gives a means of taking it into account.

The void fraction at transition is available from these

experiments only for air and water. But the fact that the steam-water data correlated successfully suggests that the void at transition lies between 80 and 90% for these and other materials as well, even though the density ratio is very different from that of the air-water combination.

5. CONCLUSIONS

The conclusions are summarized as follows:

1. For sufficiently low liquid velocities, the annular-semiannular transition can be represented by

$$V_g^{*+} = 0.9 + 0.6\, V_f^{*} \qquad (V_f^{*} < 1.0). \tag{19}$$

2. For high liquid velocities the transtion line is a line of constant quality, empirically given by

$$V_{g_s}^{+} = \left(7 + .06\, \frac{\rho_f}{\rho_g}\right) V_{f_s} \qquad (V_f^{*} \gtrsim 1.5). \tag{21}$$

3. The volume void fraction at transtion lies between 80 and 90%, the higher figure applying at zero liquid flow.
4. The transition line is uninfluenced, to first order, by reduction in liquid surface tension or introduction of substantial time variation of surface tension due to liquid impurities, if the liquid flow is small.
5. The liquid viscosity does not significantly affect the transition line.
6. There is an uncorrelated diameter effect which tends to depress the transition gas velocity for large-diameter tubes at low pressure.

BIBLIOGRAPHY

1. R. W. Lockhart and R. C. Martinelli, "Proposed Correlation of Data for Isothermal Two-Phase, Two-Component Flow in Pipes," Chemical Engineering Progress, Vol. 45, No. 1, p. 39, 1949.
2. P. Griffith and G. B. Wallis, "Two-Phase Slug Flow," ASME Journal of Heat Transfer, Vol. 83, Series C, No. 3, p. 307, 1961.
3. D. J. Nicklin, J. O. Wilkes, and J. F. Davidson, "Two-Phase Flow in Vertical Tubes," Trans. Inst. Chem. Eng., Vol. 40, p. 61, 1962.
4. D. J. Nicklin and J. F. Davidson, "The Onset of Instability in Two-Phase Slug Flow," Symposium on Two-Phase Fluid Flow, arranged by the Institution of Mechanical Engineers, Session 1, Paper 4, February 7, 1962.
5. M. Suo, "Two-Phase Flow in Capillary Tubes," Sc.D. Thesis, Massachusetts Institute of Technology, March, 1963.
6. A. D. K. Laird, "Stability Considerations in Vertical Annular Two-Phase Flow," Ph.D. Thesis, University of California, 1951.
7. S. Calvert and B. Williams, "Upward Cocurrent Flow of Air and Water in Smooth Tubes," A.I.Ch.E. Journal, Vol. 1, No. 1, pp. 78-86, 1955.
8. G. W. Govier, B. A. Radford, and J. S. C. Dunn, "The Upwards Vertical Flow of Air-Water Mixtures," Canadian Journal of Chemical Engineering, p. 58, August, 1957.

9. D. A. Charvonia, "A Review of the Published Literature Pertaining to the Annular, Two-Phase Flow of Liquid and Gaseous Media in a Pipe," Project Squid Technical Report PUR - 32 - R, Purdue University, December, 1958.

10. G. B. Wallis, "Flooding Velocities for Air and Water in Vertical Tubes," AEEW - R 123, AEE Winfrith, 1962.

11. G. B. Wallis, "The Transition from Flooding to Upwards Cocurrent Annular Flow in a Vertical Pipe," AEEW - R 142, AEE Winfrith, 1962.

12. G. B. Wallis, D. A. Steen, S. N. Brenner, and J. M. Turner, Joint U. S. - Euratom Research and Development Program, Contract No. AT (30-1) - 3114, Quarterly Progress Report, Dartmouth College, January, 1964.

13. G. B. Wallis, "The Onset of Droplet Entrainment in Annular Gas-Liquid Flow," Report No. 62 GL 127, General Engineering Laboratory, General Electric Co., August, 1962.

14. G. B. Wallis, D. A. Steen, and S. N. Brenner, Joint U. S. - Euratom Research and Development Program, Contract No. AT (30-1) - 3114, Quarterly Progress Report, Dartmouth College, July, 1963.

15. J. V. Solomon, "Construction of a Two Phase Flow Regime Transition Detector," S. M. Thesis, Massachusetts Institute of Technology, June, 1962.

16. W. A. Leary and D. H. Tsai, "Metering of Gases by Means of the A.S.M.E. Square-Edged Orifice with Flange Taps," Sloan Laboratory, Massachusetts Institute of Technology, July, 1951.

17. G. B. Wallis, personal communication, August, 1963.

18. P. Griffith, "The Slug-Annular Flow Regime Transition at Elevated Pressure," AEC Research and Development Report ANL - 6796, Argonne National Laboratory, November, 1963.

19. G. F. Hewitt and G. B. Wallis, "Flooding and Associated Phenomena in Falling Film Flow in a Tube," AERE - R 4022, AERE, Harwell, 1963.

NOMENCLATURE

English Letters

A	cross-sectional area of pipe (ft^2)
D	inside diameter of pipe (ft)
f	friction factor, defined in Eqs. (9) and (10), (dimensionless)
g	acceleration of gravity (ft/sec^2)
g_c	unit conversion constant of 32.2 $\#_m$ ft/$\#sec^2$
K	undetermined function of α, $\frac{\rho_f}{\rho_g}$, V_f^* (dimensionless)
L	length of test pipe (ft)
P	dimensionless pressure drop defined in Eq. (18)
p	pressure ($\#/ft^2$)
Q	volume rate of fluid flow (ft^3/sec)
r	radius measured from center of pipe (ft)
V	velocity averaged across section (ft/sec)
V_{f_s}, V_{g_s}	superficial velocities of liquid and gas, defined as Q_f/A and Q_g/A (ft/sec)
z	distance upward from bottom of control volume (ft)

Greek Letters

α	volume void fraction averaged over length of control volume (dimensionless)
μ	dynamic viscosity ($\#_m$/ft sec)
ρ	mass density ($\#_m/ft^3$)
σ	surface tension (#/ft)
τ	shear stress ($\#/ft^2$)

Subscripts

d	denotes special use of downflow in Eq. (2)
f	denotes liquid
g	denotes gas
i	denotes gas-liquid interface
o	denotes tube wall
s	denotes "superficial"

Superscripts

*	denotes dimensionless gas and liquid flow parameters defined by Eqs. (3) and (4)
+	denotes value at transition

APPENDIX A

Measured Values for Two Components at Low Pressure

Note that in the "Regime" column the abbreviations are as follows:

a	indicates "definitely annular"
la	indicates "low annular"
hs	indicates "high semiannular"
s	indicates "definitely semiannular"

Velocities are in (ft/sec), pressure drops are in (in Hg/ft), and voids are dimensionless. A blank in the void column indicates that no measurement was made.

Table A. 1. 0.5" I.D. tube, air and city water. $\frac{\rho_f}{\rho_g} \doteq 740$

No.	V_{f_s}	V_{g_s}	(-dp/dz)	α	Regime
1	.792	202.	2.34	.959	a
2	1.36	177.5	2.25	.932	a
3	1.55	152.5	2.12	.900	a
4	1.228	119.8	1.91	.892	a
5	1.497	92.3	1.40	.868	a
6	1.34	73.4	1.14	.847	a
7	1.292	57.8	.87	.830	la
8	1.45	26.6	.56	.745	s
9	1.755	147.1	3.16	.899	a
10	2.30	131.2	2.93	.881	a
11	1.885	120.5	2.48	.880	la
12	1.988	113.5	2.49	.871	la
13	2.88	106.8	2.36	.854	s
14	3.26	87.4	2.42	.838	s
15	3.55	62.8	2.14	.789	s
16	5.48	24.9	1.79	.658	s
17	1.63	102.2	1.77		a
18	1.86	87.7	1.70		hs
19	1.14	92.8	1.28		a
20	1.46	74.1	1.21		a
21	.37	76.0	.48		a
22	.40	47.5	.33		la
23	2.15	143.5	3.49		a
24	2.38	132.5	3.48		la
25	.03	53.3	.12		a
26	.031	23.0	.121		hs
27	.268	68.5	.204		a
28	.261	38.5	.204		la

Table A. 1., continued

No.	V_{f_s}	V_{g_s}	(-dp/dz)	α	Regime
29	1.305	76.1	1.070		a
30	1.607	59.6	1.033		la
31	1.420	94.4	1.472		a
32	1.850	72.5	1.371		hs
33	.00	37.9	.097		la
34	.00	21.9	.097		s
35	.458	77.4	.497		a
36	.412	60.4	.387		a
37	1.230	89.1	1.205		a
38	1.435	74.5	1.205		a
39	1.450	108.5	1.835		a
40	1.865	88.7	1.772		hs
41	.582	83.4	.650		a
42	.603	64.9	.522		a
43	.740	87.8	.828		a
44	.818	73.8	.708		a
45	.0795	106.8	.249	.956	a
46	.0338	91.6	.153	.957	a
47	.319	85.4	.436	.921	a
48	.410	76.1	.438	.910	a
49	.312	52.2	.277	.887	la
50	.253	29.1	.179	.838	s
51	.236	20.9	.198	.809	s
52	.283	9.49	.163	.784	s
53	1.052	140.8	1.96	.926	a
54	1.25	124.5	1.86	.909	a
55	1.535	106.2	1.83	.882	a
56	1.665	92.8	1.76	.863	la
57	2.05	82.6	1.78	.839	hs
58	2.56	63.6	1.69	.809	s
59	3.31	41.8	1.59	.758	s
60	2.09	137.6	3.31		a
61	2.27	129.9	3.23		la
62	2.56	119.2	3.23		hs
63	2.75	109.5	3.13		s
64	1.75	132.8	2.97		a
65	2.19	121.0	2.90		la
66	2.42	108.6	2.81		hs
67	2.73	98.8	2.75		s
68	1.73	117.5	2.46		a
69	1.86	111.3	2.32		la
70	2.19	96.4	2.24		hs
71	2.45	85.5	2.17		s
72	1.55	110.4	1.94		a
73	1.64	107.0	1.911		la
74	1.98	87.5	1.845		hs
75	2.26	76.0	1.805		s
76	1.34	100.	1.55		a

Table A. 1., continued

No.	V_{f_s}	V_{g_s}	(-dp/dz)	α	Regime
77	1.62	85.8	1.499		la
78	2.01	67.6	1.425		hs
79	2.26	57.4	1.36		s
80	1.35	87.0	1.336		a
81	1.61	72.5	1.275		la
82	2.05	58.1	1.218		hs
83	2.31	45.1	1.128		s
84	1.12	75.9	1.007		a
85	1.37	60.5	.921		la
86	1.66	36.7	.784		hs
87	1.78	25.9	.685		s
88	.50	66.7	.482		a
89	.535	46.1	.396		la
90	.56	21.7	.336		hs
91	.56	18.1	.325		s
92	1.46	77.4	1.288		a
93	1.64	69.8	1.235		la
94	1.97	55.4	1.175		hs
95	2.11	48.4	1.150		s
96	1.30	77.3	1.124		a
97	1.48	67.3	1.107		la
98	1.81	51.0	1.028		hs
99	1.98	43.0	.986		s
100	2.47	155.	4.80		a
101	2.76	149.	4.56		la
102	3.29	125.6	4.37		hs
103	3.60	115.2	4.27		s
104	2.17	143.	3.65		a
105	2.41	133.	3.56		la
106	2.68	122.	3.48		hs
107	2.83	115.2	3.40		s
108	2.06	132.	3.06		a
109	2.28	121.4	2.99		la
110	2.47	112.4	2.92		hs
111	2.62	106.2	2.86		s
112	.87	75.8	.906		a
113	.99	65.8	.794		la
114	1.23	32.4	.598		hs
115	1.31	22.5	.532		s
116	.29	67.7	.323		a
117	.30	43.2	.263		la
118	.21	26.6	.247		hs
119	.20	15.9	.275		s
120	.47	76.5	.505		a
121	.50	50.5	.387		la
122	.51	33.3	.338		hs
123	.49	21.7	.345		s
124	.66	81.8	.734		a

Table A. 1., continued

No.	V_{f_s}	V_{g_s}	(-dp/dz)	α	Regime
125	.80	54.3	.593		1a
126	.85	35.1	.501		hs
127	.89	23.7	.480		s
128	1.15	90.5	1.231		a
129	1.55	69.3	1.160		1a
130	1.77	60.2	1.123		hs
131	2.03	48.0	1.059		s
132	.572	76.5	.591	.902	a
133	.678	17.25	.389	.757	s
134	2.22	138.8	3.35	.889	a
135	2.96	106.5	3.09	.859	s

Table A. 2. 0.5" I.D. pipe, air and city water + alcohol $\frac{\rho_f}{\rho_g} \doteq 740.$
With 2 1/2% methyl alcohol, $\sigma \doteq 66$ dynes/cm
With 5% ethyl alcohol, $\sigma \doteq 57$ dynes/cm

No.	V_{f_s}	V_{g_s}	(-dp/dz)	α	Regime	σ
1	2.03	133.5	2.91	.888	a	66.
2	2.03	131.8	2.85	.887	1a	66.
3	2.10	126.2	2.57	.882	hs	66.
4	2.15	106.8	2.32	.857	s	66.
5	.649	61.5	.547	.884	1a	56.1
6	.649	25.6	.380	.802	hs	56.3
7	1.20	105.6	1.548	.903	a	56.8
8	1.262	56.1	.869	.853	hs	57.0
9	.870	68.3	.814	.878	1a	57.4
10	.865	29.5	.505	.790	hs	57.4

Table A. 3. 0.5" I.D. pipe, air and city water + glycerine $\frac{\rho_f}{\rho_g} \doteq 788$, $\mu \doteq 1.92$ cp

No.	V_{f_s}	V_{g_s}	(-dp/dz)	α	Regime
1	1.14	65.6	.930	.850	la
2	1.15	37.0	.635	.817	hs
3	1.61	94.7	1.679	.856	la
4	1.59	58.4	1.085	.812	hs
5	1.98	115.2	2.41	.867	la
6	2.05	93.8	1.958	.848	hs
7	2.44	127.1	3.28	.874	la
8	2.51	114.7	2.95	.859	hs
9	.043	34.4	.162	.887	la
10	0.0	18.3	.190	.835	hs
11	.15	48.8	.221	.900	la
12	.144	23.5	.225	.839	hs

Table A. 4. 0.5" I.D. pipe, carbon dioxide and city water $\frac{\rho_f}{\rho_g} \doteq 484$

No.	V_{f_s}	V_{g_s}	(-dp/dz)		Regime
1	.388	70.6	.500	.923	a
2	.456	36.1	.357	.863	la
3	.465	23.2	.322	.793	hs
4	.454	17.05	.332	.766	s
5	.576	58.7	.544		a
6	.618	50.4	.495	.879	la
7	.757	21.3	.424	.767	hs
8	.784	17.45	.416	.759	s
9	1.382	78.2	1.42	.870	a
10	1.785	61.9	1.37	.825	la
11	2.21	47.1	1.285	.777	hs
12	2.44	40.0	1.21	.768	s
13	2.37	59.5	3.26		a
14	2.54	62.2	2.99	.856	la
15	3.24	69.9	2.78	.840	hs
16	2.52	71.6	2.55	.864	la
17	2.94	91.9	2.43	.814	hs
18	2.26	96.5	2.34		la

Table A. 5. 1.0" I.D. pipe, air and city water, $\frac{\rho_f}{\rho_g} \doteq 830$

No.	V_{f_s}	V_{g_s}	(-dp/dz)	α	Regime
1	.00	29.7	.0645	.910	a
2	.00	27.7		.895	la
3	.00	25.9		.889	hs
4	.00	23.8		.878	s
5	.206	53.2	.132	.923	a
6	.196	41.1	.118	.904	la
7	.180	28.1	.138	.855	s
8	.530	51.0	.225	.886	a
9	.510	48.8	.217	.882	a
10	.457	46.1	.193	.879	la
11	.463	36.7	.187	.855	hs
12	.501	26.1	.207	.813	s
13	.830	60.9	.341	.879	a
14	.832	57.0	.338	.870	la
15	.841	53.4	.322	.863	la
16	.860	43.1	.293	.837	hs
17	1.102	65.7	.448	.867	a
18	1.10	63.9	.460	.869	a
19	1.13	59.6	.421	.856	la
20	1.14	54.3	.421	.849	hs
21	1.18	42.6	.407	.816	s
22	1.400	77.2	.60	.871	a
23	1.400	72.1	.565	.865	la
24	1.42	65.3	.546	.855	hs
25	1.47	53.5	.495	.836	s
26	.532	79.0	.300	.926	a
27	.510	75.8	.286	.920	a
28	.484	68.5	.240	.913	a
29	.655	57.8	.281	.888	a
30	.179	87.0	.174	.957	a
31	.1645	80.0	.152	.953	a
32	.1640	72.1	.1345	.950	a
33	.1590	61.3	.1113	.943	a
34	.1542	45.5	.0976	.922	a
35	.0192	48.5	.0448	.952	a
36	.0132	40.6	.0487	.943	a
37	.00	32.0	.0663	.918	a
38	.01	52.8	.0332	.962	a

Table A. 6. 1.0" I.D. pipe, air and water + methyl alcohol (2 1/2%)

$\frac{\rho_f}{\rho_g} \doteq 830$, $\sigma \doteq 66$ dynes/cm

No.	V_{f_s}	V_{g_s}	(-dp/dz)	α	Regime
1	.816	50.8	.299	.864	a
2	.788	45.7	.266	.857	s

Table A. 7. 1.0" I.D. pipe, air and water + glycerine (25%)

$\frac{\rho_f}{\rho_g} \doteq 830$, $\mu = 1.92$ cp

No.	V_{f_s}	V_{g_s}	(-dp/dz)	α	Regime
1	1.050	55.0	.694	.849	la
2	1.046	47.7	.570	.835	s
3	.493	44.9	.230	.870	a
4	.493	30.4	.226	.825	s
5	.493	40.8	.222	.860	la
6	.492	36.5	.213	.847	hs

Table A. 8. 1.5" I.D. pipe, air and city water, $\frac{\rho_f}{\rho_g} \doteq 830$

No.	V_{f_s}	V_{g_s}	(-dp/dz)	α	Regime
1	.412	42.8	.1660	.876	a
2	.418	41.6	.1540	.868	a
3	.430	38.5	.1660	.859	a
4	.436	36.3	.1720	.850	a
5	.448	32.8	.1580	.842	a
6	.458	30.7	.1819	.827	la or hs
7	.641	40.3	.1895	.826	la
8	.666	29.0	.227	.808	hs
9	.688	21.9	.217	.798	hs
10	.688	18.3	.255	.786	s
11	.703	7.95	.264	.736	s
12	.718	5.41	.239	.671	s
13	.641	1.66	.385	.500	slug flow

Table A. 8., continued

No.	V_{f_s}	V_{g_s}	(-dp/dz)	α	Regime
14	1.188	47.1	.302	.841	a
15	1.188	46.0	.314	.828	la
16	1.188	42.0	.302	.830	hs
17	1.231	37.9	.282	.817	s
18	.0299	47.1	.0434	.947	a
19	.0368	44.1	.0256	.939	a
20	.0354	39.3	.0652	.925	a
21	.0344	36.4	.0612	.913	a
22	.0323	33.1	.0830	.897	a
23	.0291	30.1	.0988	.883	la
24	.0253	21.6	.1184	.841	hs
25	.0229	18.6	.1421	.826	s
26	.1373	59.8	.0770	.945	a
27	.1578	52.5	.0790	.933	a
28	.1641	45.1	.0948	.916	a
29	.1650	40.2	.0967	.901	a
30	.1690	35.2	.1007	.881	la
31	.1722	32.1	.1242	.868	la
32	.1758	28.0	.1381	.851	la or hs
33	.1740	24.4	.1600	.830	hs
34	.1758	18.4	.1757	.798	s
35	.805	50.2	.227	.862	a
36	.830	47.4	.233	.854	a
37	.844	44.6	.205	.851	la
38	.873	39.1	.239	.833	la or hs
39	.918	36.8	.292	.829	hs
40	.935	34.3	.267	.814	s
41	.952	30.8	.267	.802	s
42	.969	27.3	.251	.790	s
43	.969	23.6	.269	.768	s
44	.988	18.95	.302	.751	s
45	1.025	11.82	.281	.711	s
46	1.006	2.2	.381	.517	slug flow

APPENDIX B

The raw data of Reference (19) are reproduced here by courtesy of Professor Griffith. The superficial velocities are in (ft/sec). No void or pressure drop data were taken. The regime probe and circuit were the same as those used for the low-pressure, two-component tests with slight modifications for operation at higher pressure and temperature.

Table B. 1. 0.375" I.D. tube, steam and water at 200 psig, $\frac{\rho_f}{\rho_g}$ =115.6

No.	V_{f_s}	V_{g_s}	Regime	No.	V_{f_s}	V_{g_s}	Regime
1	7.4	56.5	s	15	4.9	89.	a
2	6.1	71.5	s	16	5.1	71.	hs
3	5.65	85.5	hs	17	5.6	4.6	s
4	4.35	29.3	s	18	5.3	33.3	s
5	4.35	46.0	hs	19	5.2	51.	s
6	3.85	58.0	la	20	4.8	72.5	la
7	3.75	68.5	a	21	4.16	74.	a
8	15.4	13.	s	22	5.1	54.	hs
9	10.0	42.5	s	23	3.06	17.2	s
10	7.3	23.	s	24	3.4	36.4	hs
11	7.3	35.	s	25	3.02	54.5	la
12	6.3	50.	s	26	2.96	60.5	a
13	5.8	66.	hs	27	3.1	43.7	la
14	4.95	84.	la				

Table B. 2. 0.375" I.D. tube, steam and water at 400 psig, $\frac{\rho_f}{\rho_g} = 57.7$

No.	V_{f_s}	V_{g_s}	Regime	No.	V_{f_s}	V_{g_s}	Regime
1	8.67	26.7	s	15	3.2	6.0	s
2	7.7	38.0	s	16	3.1	8.7	s
3	5.65	53.5	hs	17	2.7	12.5	hs
4	4.95	59.0	hs	18	1.6	20.5	hs
5	4.95	66.0	la	19	1.2	25.0	la
6	4.90	77.0	a	20	1.1	29.4	a
7	5.92	59.0	hs	21	4.6	7.35	s
8	5.36	7.5	s	22	4.45	17.5	s
9	5.12	24.2	s	23	4.2	27.2	s
10	5.0	34.	hs	24	4.1	36.2	s
11	4.7	44.	hs	25	3.8	41.5	hs
12	4.21	47.	la	26	3.46	46.5	la
13	3.86	61.5	a	27	3.0	63.1	a
14	3.24	72.	a				

Table B. 3. 0.375" I.D. pipe, steam and water at 600 psig, $\frac{\rho_f}{\rho_g} = 37.1$

No.	V_{f_s}	V_{g_s}	Regime	No.	V_{f_s}	V_{g_s}	Regime
1	3.56	22.6	s	9	6.3	52.0	hs
2	3.41	30.4	hs	10	5.5	58.0	la
3	3.3	33.6	hs	11	5.05	69.0	a
4	3.12	43.6	la	12	5.3	30.6	s
5	3.07	49.0	a	13	4.65	43.6	hs
6	9.75	19.1	s	14	4.36	48.6	la
7	8.70	25.0	s	15	3.87	56.5	a
8	7.04	42.5	s				

Table B. 4. 0.625" I.D. pipe, steam and water at 200 psig, $\frac{\rho_f}{\rho_g} = 115.6$

No.	V_{f_s}	V_{g_s}	Regime	No.	V_{f_s}	V_{g_s}	Regime
1	6.0	27.4	s	13	3.84	61.5	a
2	6.0	34.6	s	14	4.02	43.0	la
3	6.0	41.6	hs	15	3.14	17.3	s
4	6.0	47.5	hs	16	3.05	27.3	hs
5	4.95	24.4	s	17	3.00	39.4	la
6	4.75	37.5	hs	18	2.98	49.6	a
7	4.60	47.6	la	19	3.02	32.8	hs
8	4.50	58.0	la	20	1.70	17.8	s
9	4.65	42.2	hs	21	1.63	23.6	hs
10	4.16	27.8	s	22	1.60	28.9	la
11	4.08	39.2	hs	23	1.53	39.7	a
12	4.00	49.5	la	24	1.68	19.3	hs

Table B. 5. 0.625" I.D. pipe, steam and water at 400 psig, $\frac{\rho_f}{\rho_g} = 57.7$

No.	V_{f_s}	V_{g_s}	Regime	No.	V_{f_s}	V_{g_s}	Regime
1	1.6	6.7	s	15	3.40	35.2	la
2	1.66	12.1	s	16	3.22	41.2	a
3	1.60	15.7	hs	17	3.45	31.8	hs
4	1.50	19.1	la	18	4.85	21.9	s
5	1.48	22.7	la	19	4.70	28.0	s
6	1.43	24.3	a	20	4.5	34.7	hs
7	3.05	11.8	s	21	4.3	41.1	la
8	2.80	24.6	hs	22	4.2	45.9	a
9	2.75	28.4	la	23	3.52	65.8	a
10	2.70	34.7	a	24	5.44	27.2	s
11	2.80	25.0	hs	25	5.29	34.5	s
12	3.8	16.1	s	26	5.01	42.6	hs
13	3.7	22.0	hs	27	4.86	55.0	la
14	3.55	28.4	hs	28	4.60	66.8	a

Table B. 6. 0.625" I.D. pipe, steam and water at 600 psig, $\frac{\rho_f}{\rho_g}$ = 37.1

No.	V_{f_s}	V_{g_s}	Regime	No.	V_{f_s}	V_{g_s}	Regime
1	5.6	19.2	s	20	3.42	26.4	hs
2	5.5	23.2	s	21	3.0	63.5	s
3	5.2	29.6	hs	22	2.86	11.2	s
4	5.06	32.8	hs	23	2.75	15.3	hs
5	4.84	37.4	hs	24	2.62	20.0	hs
6	4.71	42.4	la	25	2.52	24.2	la
7	4.6	15.1	s	26	2.36	29.8	a
8	4.5	19.5	s	27	2.58	21.9	la
9	4.36	24.3	hs	28	1.65	5.39	s
10	4.23	29.2	hs	29	1.51	11.1	hs
11	4.16	32.8	la	30	1.38	15.7	la
12	4.02	37.0	a	31	1.26	20.4	a
13	3.99	38.2	a	32	1.48	12.5	hs
14	4.18	31.6	hs	33	1.11	2.02	s
15	3.74	15.6	s	34	1.00	4.48	s
16	3.64	19.7	hs	35	.86	6.96	hs
17	3.52	24.2	hs	36	.74	9.0	la
18	3.34	30.8	la	37	.71	10.5	a
19	3.31	32.9	a	38	.76	8.1	la

Table B. 7. 0.875" I.D. tube, steam and water at 200 psig, $\frac{\rho_f}{\rho_g}$ = 115.6

No.	V_{f_s}	V_{g_s}	Regime	No.	V_{f_s}	V_{g_s}	Regime
1	.645	10.0	s	6	.53	23.3	hs
2	.62	12.0	s	7	.51	25.8	la
3	.61	14.8	s	8	.49	27.4	la
4	.58	17.5	hs	9	.455	32.1	a
5	.55	20.3	hs	10	2.65	6.32	s

Table B. 7., continued

No.	V_{f_s}	V_{g_s}	Regime	No.	V_{f_s}	V_{g_s}	Regime
11	2.58	14.9	s	23	1.75	8.7	s
12	2.51	21.8	s	24	1.69	15.0	s
13	2.48	25.1	hs	25	1.64	21.0	s
14	2.44	30.4	hs	26	1.59	26.5	la
15	2.40	34.3	la	27	1.54	32.6	a
16	2.41	33.6	la	28	1.63	21.6	hs
17	2.18	8.7	s	29	1.19	5.87	s
18	2.13	14.9	s	30	1.11	14.8	s
19	2.08	20.4	hs	31	1.08	20.1	hs
20	2.04	25.6	hs	32	1.04	25.4	la
21	1.99	30.8	la	33	1.06	22.7	la
22	1.96	34.2	a				

Table B. 8. 0.875" I.D. tube, steam and water at 400 psig, $\frac{\rho_f}{\rho_g} = 57.7$

No.	V_{f_s}	V_{g_s}	Regime	No.	V_{f_s}	V_{g_s}	Regime
1	1.94	5.23	s	14	.74	16.2	a
2	1.88	8.35	s	15	2.54	11.6	s
3	1.82	11.7	s	16	2.48	14.6	s
4	1.77	15.0	s	17	2.43	17.8	hs
5	1.71	18.4	hs	18	2.38	21.1	hs
6	1.66	21.2	la	19	2.32	24.4	la
7	1.60	24.4	a	20	2.28	27.1	a
8	1.69	19.2	la	21	2.37	21.4	hs
9	.87	8.7	s	22	2.21	8.5	s
10	.84	10.2	s	23	2.15	11.4	s
11	.82	11.7	hs	24	2.10	14.1	hs
12	.79	13.1	hs	25	2.02	18.5	hs
13	.77	14.4	la	26	1.95	21.6	la

Table B. 8., continued

No.	V_{f_s}	V_{g_s}	Regime	No.	V_{f_s}	V_{g_s}	Regime
27	1.88	24.4	a	32	1.55	19.7	hs
28	1.98	19.5	hs	33	1.53	21.2	la
29	1.73	9.67	s	34	1.48	24.1	a
30	1.70	11.9	s	35	1.56	19.5	la
31	1.66	14.0	hs				

Table B. 9. 0.875" I.D. tube, steam and water at 600 psig, $\frac{\rho_f}{\rho_g} = 37.1$

No.	V_{f_s}	V_{g_s}	Regime	No.	V_{f_s}	V_{g_s}	Regime
1	2.04	8.5	s	18	0.75	14.1	a
2	2.01	9.5	s	19	0.82	11.7	la
3	1.95	11.5	s	20	2.39	9.3	s
4	1.87	13.6	hs	21	2.32	11.8	s
5	1.82	15.6	la	22	2.26	14.4	s
6	1.74	17.6	a	23	2.19	17.0	hs
7	1.80	15.4	hs	24	2.14	19.4	la
8	1.37	8.4	s	25	2.07	21.9	la
9	1.31	10.8	s	26	2.16	18.2	hs
10	1.25	13.2	hs	27	2.06	5.0	s
11	1.18	15.6	la	28	1.97	8.0	s
12	1.12	17.8	a	29	1.91	10.3	s
13	1.23	13.9	hs	30	1.84	12.7	s
14	0.95	6.5	s	31	1.78	14.9	hs
15	0.91	7.95	s	32	1.72	17.2	la
16	0.86	10.4	hs	33	1.70	18.3	a
17	0.79	12.8	a	34	1.75	16.0	hs

APPENDIX C

Some Details of the Apparatus

The plexiglas pipes used in the experiments are fabricated from 6-foot lengths of extruded tubing. The sections are joined at their ends by collars, machined from the solid to provide a large diameter to fit the outside diameter of the tube as well as a shoulder at the middle which matches the tube inside diameter. The parts are "welded" together with the usual ethylene dichloride, which dissolves the plastic. End connections to the metal hardware are made with plastic flanges "welded" to the tube. Aluminum plates bearing on the flanges are bolted to the hardware. Centering of the tubes is accomplished by counterboring the holes in the quick-acting valves; the tube is free to slide in the counterbored holes. A soft rubber gasket between the flange and the surface of the valve provides for sealing and thermal expansion of the tube. The means of attachment is illustrated in the top photograph of Figure 31.

The three-way, quick-acting valves are modifications of the spool-type valve. An aluminum piston containing two holes of the same diameter as the flow tubes is translated to expose ports leading to either of the two tubes. The piston is accurately positioned by steel stops at either end of its stroke to provide a minimum of disturbance for the flow. To provide rapid isolation of the test section, a pneumatic cylinder, fed by 125 psi shop air, drives the piston. The cylinder is capable of isolating the 1.0" pipe in about 1/60 second. It is equally important that the top and bottom valves move simultaneously; this is

accomplished by sending the starting signal to both valves electrically. A solenoid on each valve moves a pilot plunger which directs air to one side of the actuating piston while opening the other side to the atmosphere for exhaust. For fine adjustment of the operating time, an air pressure regulator is attached to each valve; thus minor frictional differences between the two valves are compensated. The top photograph of Figure 31 shows the arrangement at the valve itself.

Sealing of the aluminum piston is accomplished by O-rings, and the space between the O-rings is packed with water-pump grease (left photograph in Figure 31). The main problem in building these valves was to provide a close fit between aluminum cylinder and brass valve body, while allowing enough clearance to give smooth operation and low friction. The clearance finally arrived at by trial and error is about .004". The valves will seal an air pressure of about 20 psi, which causes some problems in operation with a 0.5" tube, where the pressure at the bottom valve may reach 40 psig.

These custom-made valves are very expensive, and their poor sealing properties partially negate their value as reliable, accurate flow diverters, except for the larger pipes whose pressure drop is small. When it became apparent that they would not be satisfactory at 40 psig, two very inexpensive ($7.50 each) Worcester ball valves were substituted for each spool valve. The ball valves sealed adequately, and it is recommended that this type be used to construct isolation valves for void measurement. Care should be taken to see that there are no downward-facing flat surfaces within the valve body; otherwise bubbles of gas can be trapped within the valve, and the void fraction

measurement becomes unreliable. The right photograph of Figure 31 shows the arrangement of ball valves, which are linked together for actuation by the pneumatic cylinder.

The mixing tee where the gas and liquid are brought together is shown in Figure 32. The construction is of plastic; the two inlet tubes of 3/4" I.D. plexiglas and the 1" I.D. outlet (stem of the tee) are cemented into a drilled plexiglas block. The inlets are connected to the gas and liquid supplies by plastic hoses.

The same tee was used for all the tests, no matter what the pipe size. The choice of the arrangement was made to provide a chaotic mixing of gas and liquid, thus to avoid any tendency to promote annular flow by separating the phases artificially. As the gas and liquid meet head-on, and since the gas is usually moving much faster than the liquid, there is a tendency for the liquid to flow up one side of the tube (the side from which the gas enters) for a very short distance. At a height of a foot or two above the tee, however, the flow has the same appearance, when viewed through the tube wall, as it has at the probe about 15 feet higher. In view of the depression of the transition line for the 1.0" and 1.5" pipes, which is attributed to entrance effects, it would be desirable to perform the same tests again with some different inlets, especially now that a transition line has been established for fully developed flow as in the 0.5" pipe.

APPENDIX D

Listed below are the numbers used to plot the transition velocity, void, and pressure drop for the low-pressure, air-water experiments.

0.5" pipe, air-water, ρ_f/ρ_g = 740.

V_{f_s} (ft/sec)	$V_{g_s}^+$ (ft/sec)	α^+	$(-dp/dz)^+$ (in Hg/ft)	V_f^*	V_g^{*+}	p^+
0	28.3	.870	.11	0	.898	.1245
.2	31.6	.855	.175	.1725	.996	.1980
.5	36.5	.835	.335	.432	1.159	.379
.8	41.4	.823	.51	.690	1.315	.578
1.0	44.5	.820	.61	.863	1.412	.690
1.2	47.9	.815	.72	1.035	1.520	.815
1.5	52.9	.810	.90	1.295	1.678	1.020
1.6	54.2	.810	.96	1.380	1.721	1.088
1.83	90.0	.852	1.77	1.578	2.86	2.01
2.0	98.5	.860	2.10	1.726	3.12	2.38
2.5	123.1	.872	3.25	2.16	3.91	3.68
3.0	148.0	.880	5.00	2.59	4.70	5.66

1.0" pipe, air-water, ρ_f/ρ_g = 830.

V_{f_s} (ft/sec)	$V_{g_s}^+$ (ft/sec)	α^+	$(-dp/dz)^+$ (in Hg/ft)	V_f^*	V_g^{*+}	p^+
0	26.3	.890	.11	0	.556	.125
.180	31.5	.870	.134	.110	.665	.152
.47	39.8	.864	.183	.287	.842	.207
.86	50.9	.857	.308	.525	1.075	.349
1.14	58.9	.856	.419	.696	1.242	.475
1.40	66.3	.857	.550	.855	1.402	.623

1.5" pipe, air-water, ρ_f/ρ_g = 830.

V_{f_s}	$V_{g_s}^+$	α^+	$(-dp/dz)^+$	V_f^*	V_g^{*+}	p^+
(ft/sec)	(ft/sec)		(in Hg/ft)			
0	24.5	.858	.11	0	.425	.1245
.2	27.8	.845	.145	.1	.482	.1643
.4	31.0	.837	.17	.2	.537	.1925
.6	34.2	.834	.195	.3	.593	.221
.8	37.6	.833	.22	.4	.652	.249
1.0	40.8	.833	.26	.5	.708	.294
1.2	44.3	.834	.30	.6	.768	.340

LIST OF FIGURES

Symbols for Flow-Regime Indication

Used in Figures 8-22

- ● indicates definitely annular flow
- ◣ indicates low annular flow
- ◪ indicates high semiannular flow
- ◍ indicates definitely semiannular flow

DATA FOR NUMBERED CURVES IN FIGURES 23, 24, 28, 29 AND 30

Curve No.	Gas	Liquid	Tube Dia.	ρ_f/ρ_g
1	Air	City Water	0.5"	740.
2	Air	Water + Alcohol	0.5"	740.
3	Air	Water + Glycerine	0.5"	788.
4	CO_2	City Water	0.5"	484.
5	Air	City Water	1.0"	830.
6	Air	City Water	1.5"	830.
7	Steam	Water	0.375"	115.6
8	Steam	Water	0.375"	57.7
9	Steam	Water	0.375"	37.1
10	Steam	Water	0.625"	115.6
11	Steam	Water	0.625"	57.7
12	Steam	Water	0.625"	37.1
13	Steam	Water	0.875"	115.6
14	Steam	Water	0.875"	57.7
15	Steam	Water	0.875"	37.1

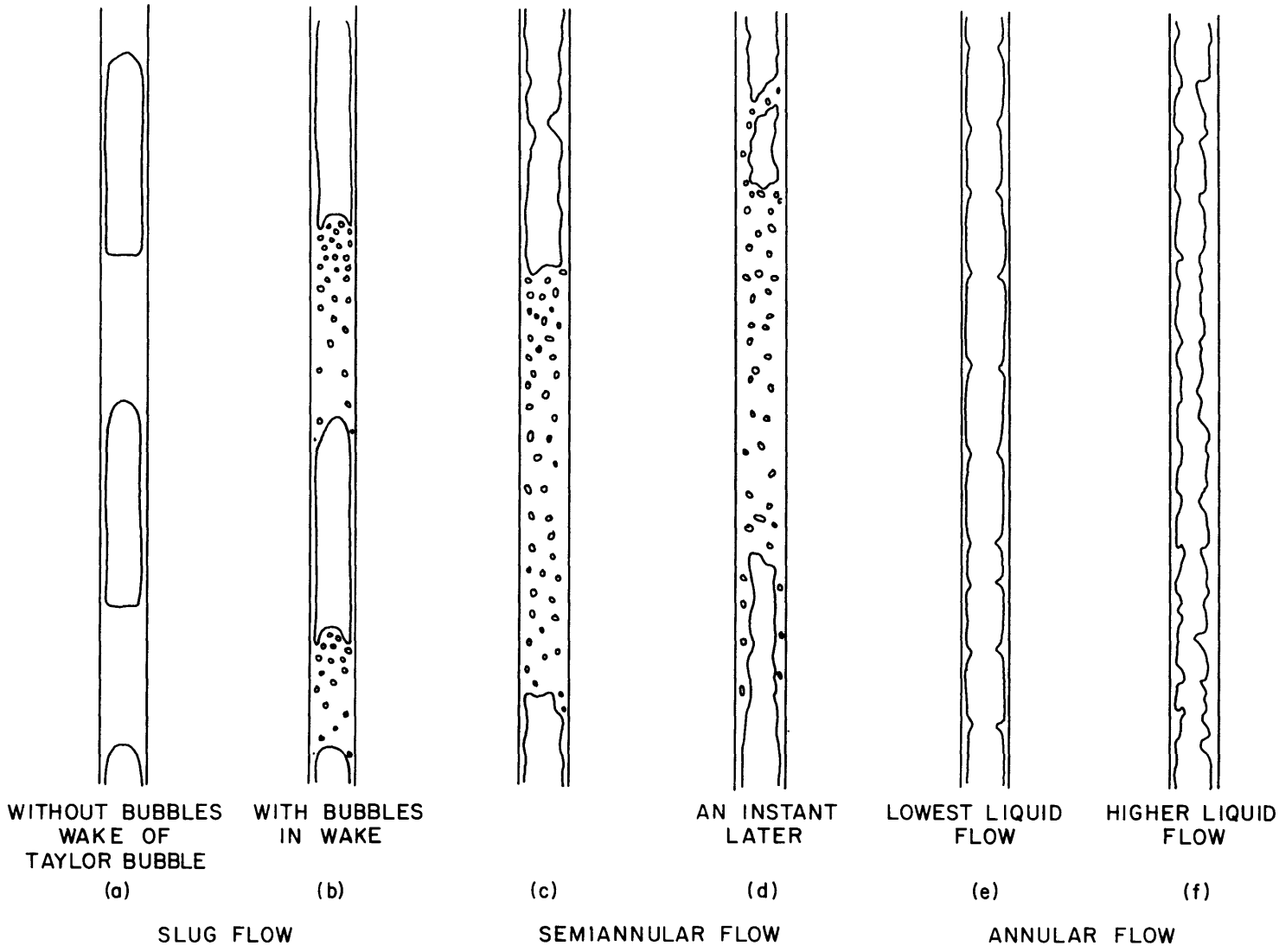

FIGURE 1 SKETCHES OF VARIOUS FLOW-REGIME GEOMETRIES

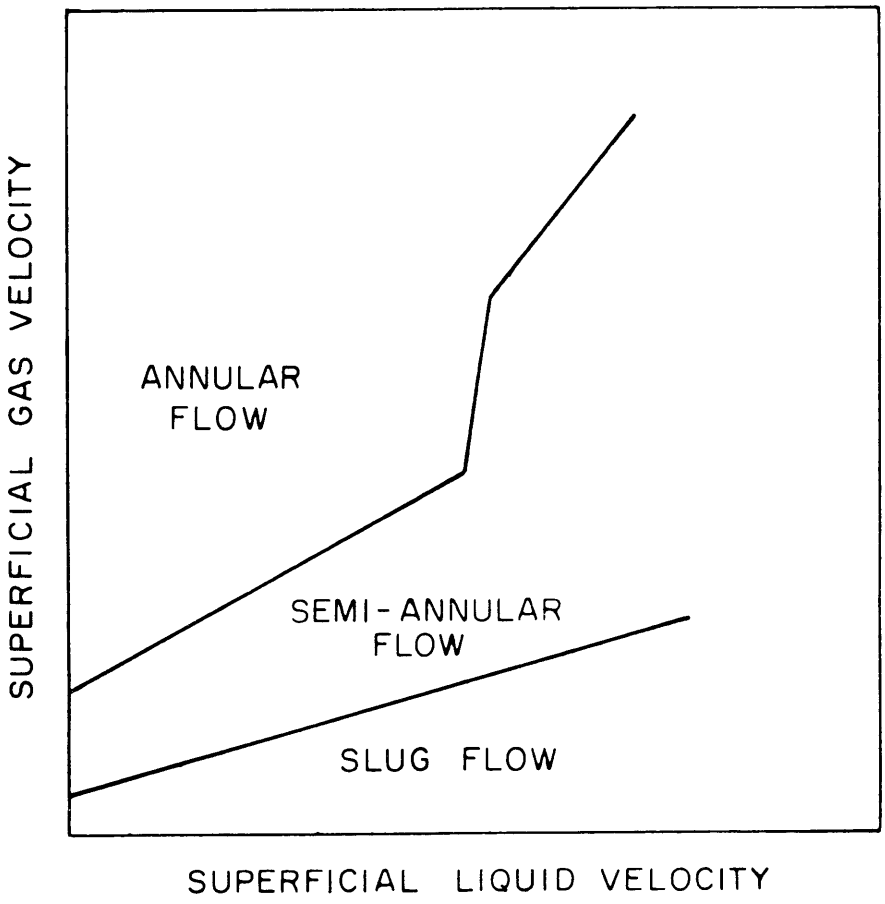

FIGURE 2 FLOW REGIMES QUALITATIVELY LOCATED

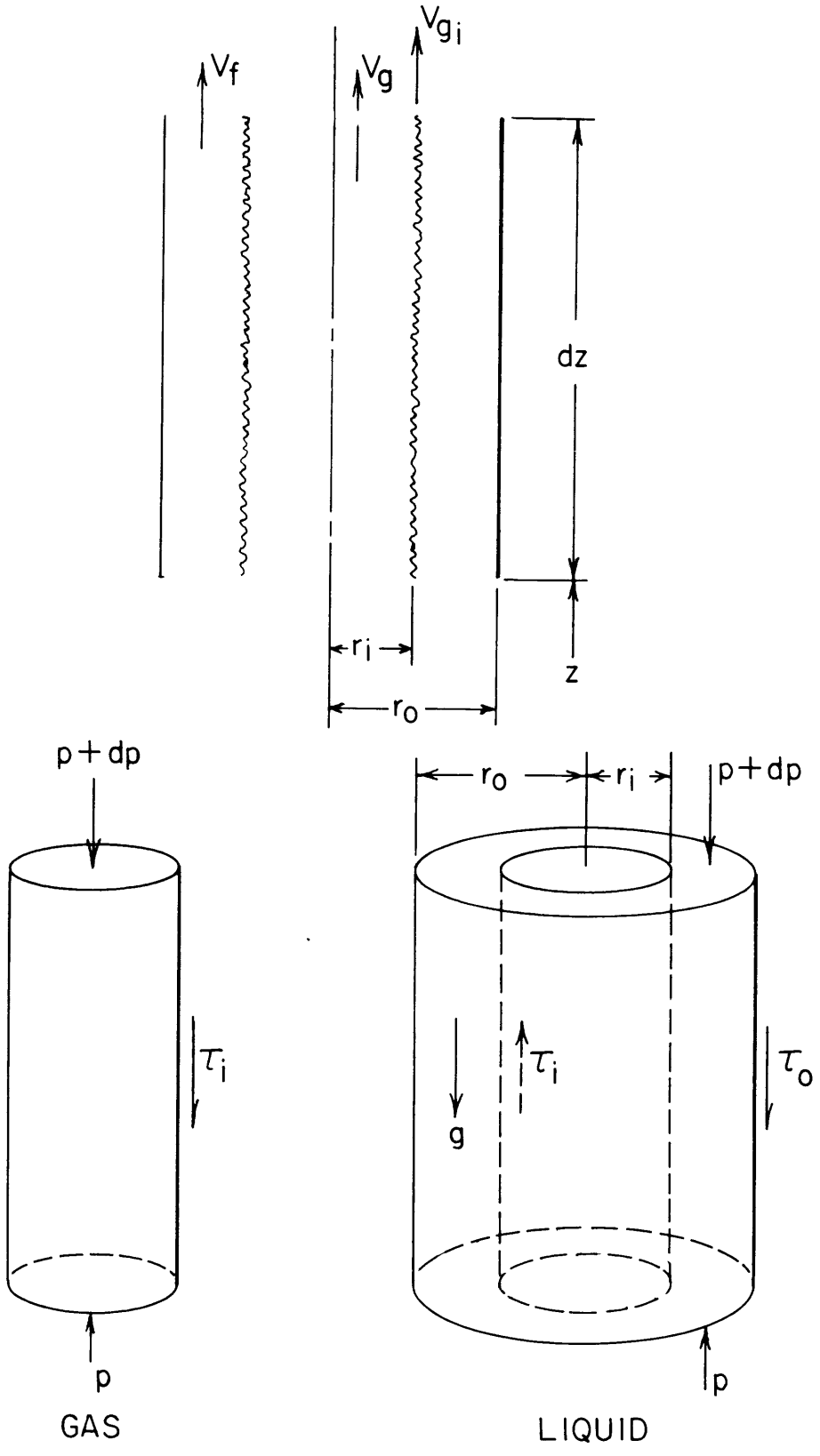

FIGURE 3 MODEL FOR ANNULAR FLOW

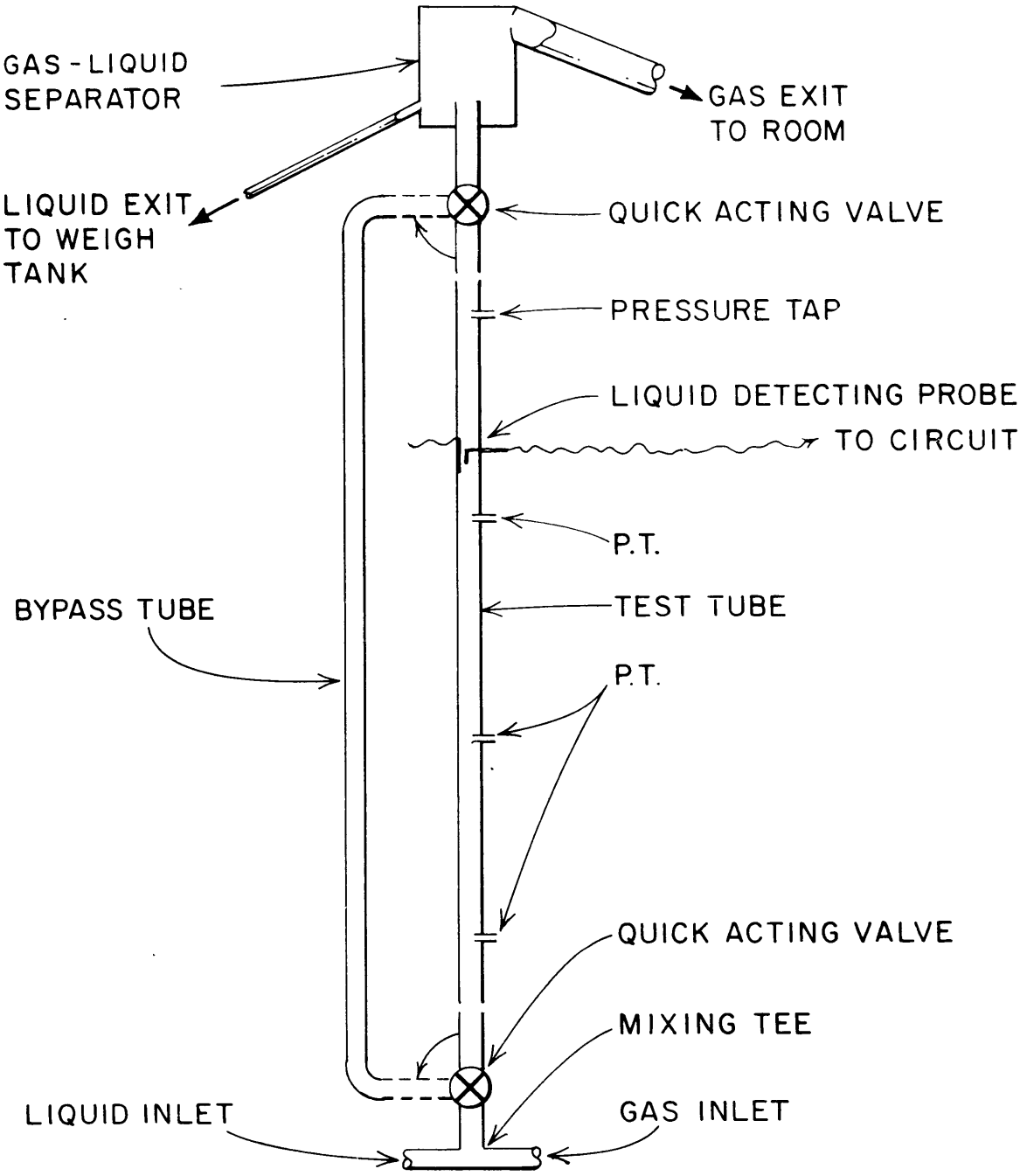

FIGURE 4 SCHEMATIC DRAWING OF TEST APPARATUS

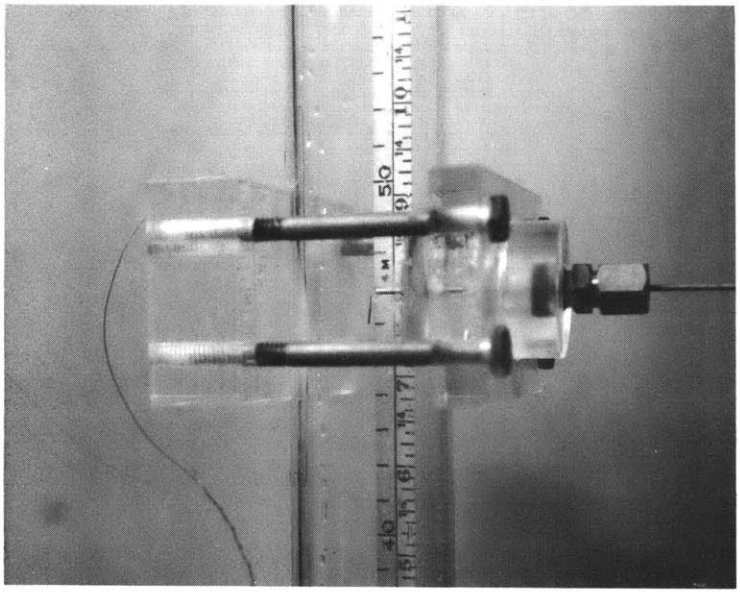

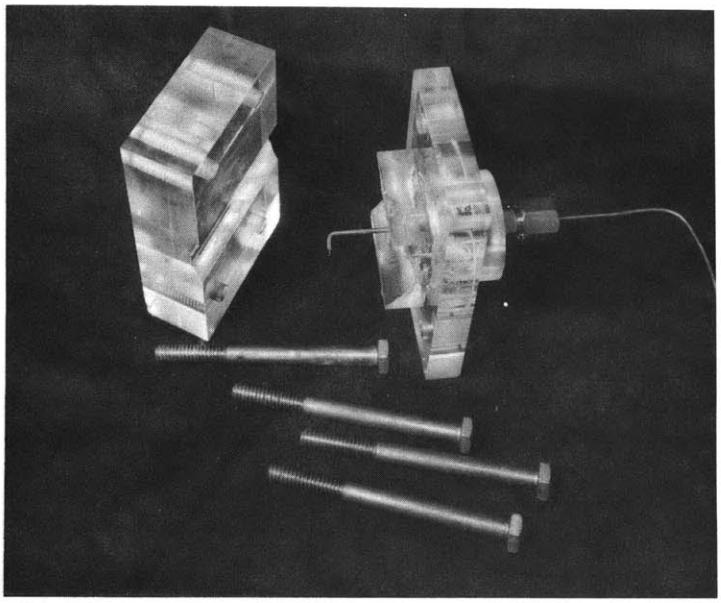

FIGURE 5

FLOW REGIME PROBE

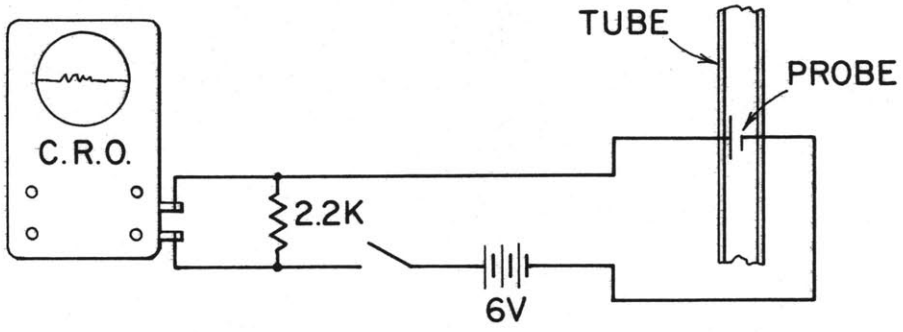

FIGURE 6 PROBE CIRCUIT

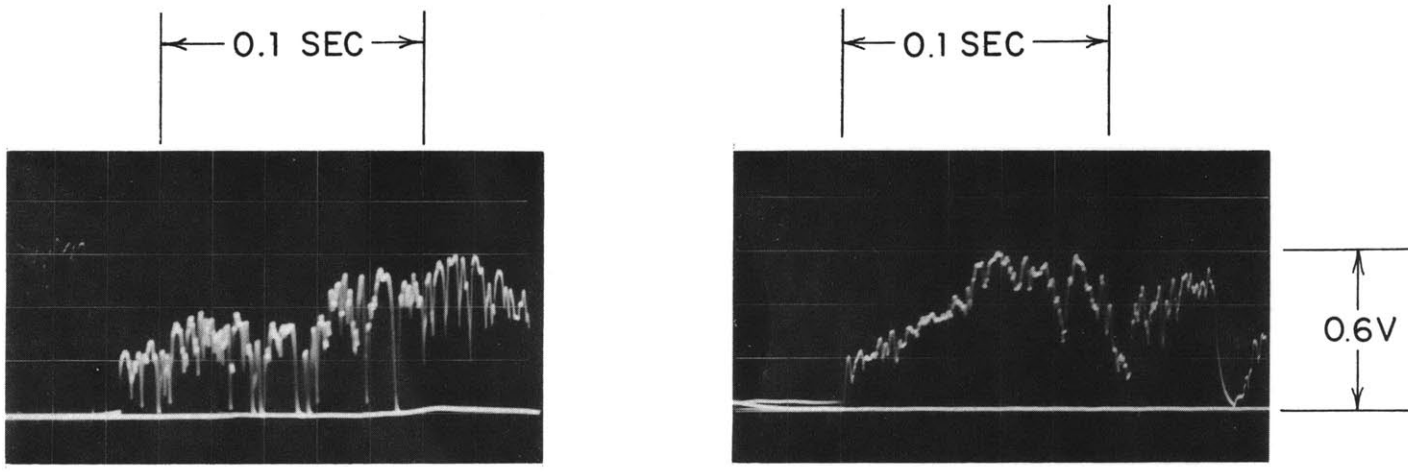

FIGURE 7 TYPICAL INDICATIONS OF SEMI-ANNULAR FLOW

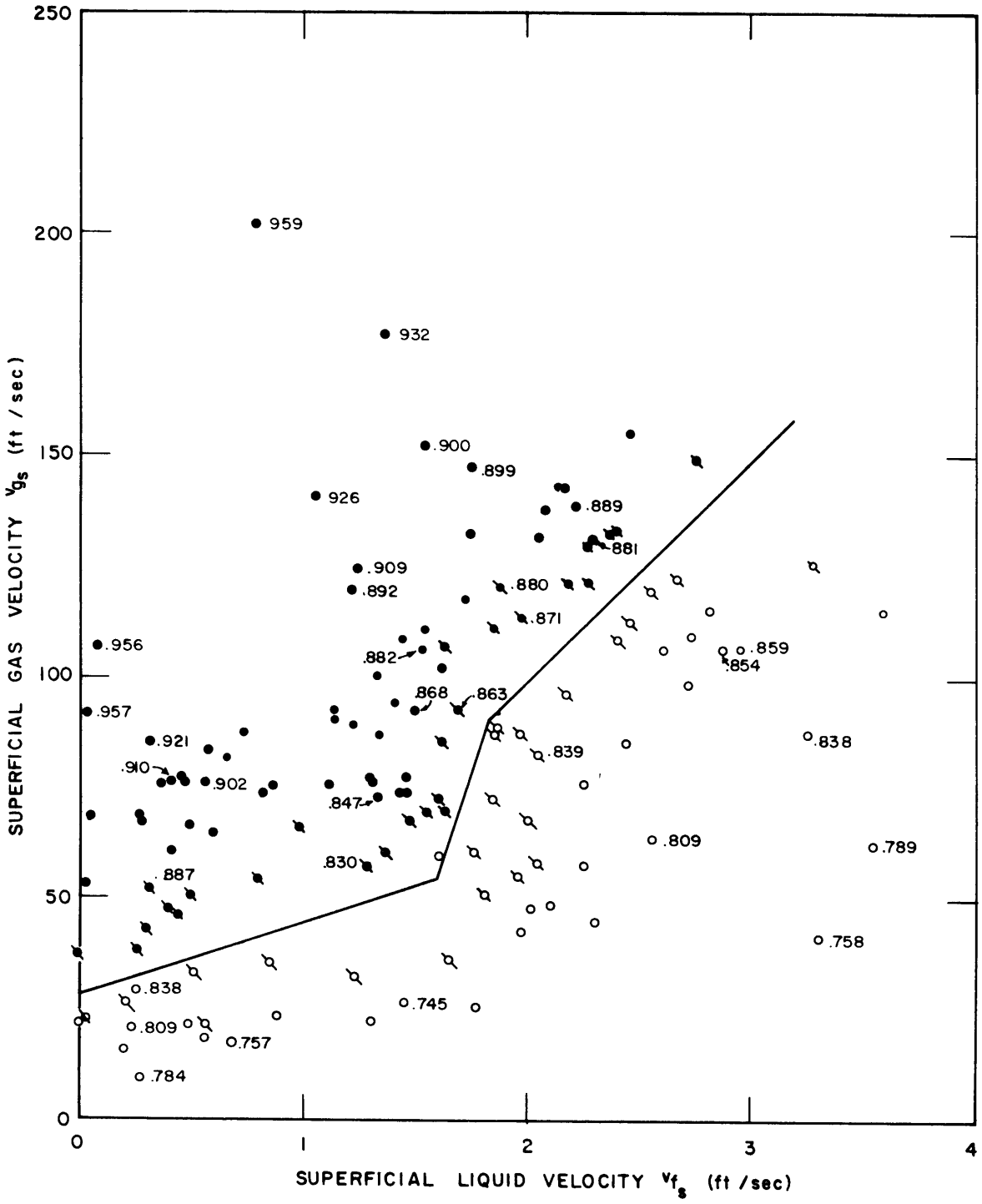

FIG. 8 TRANSITION LINE FOR AIR AND WATER, 0.5" TUBE, ATMOSPHERIC PRESSURE

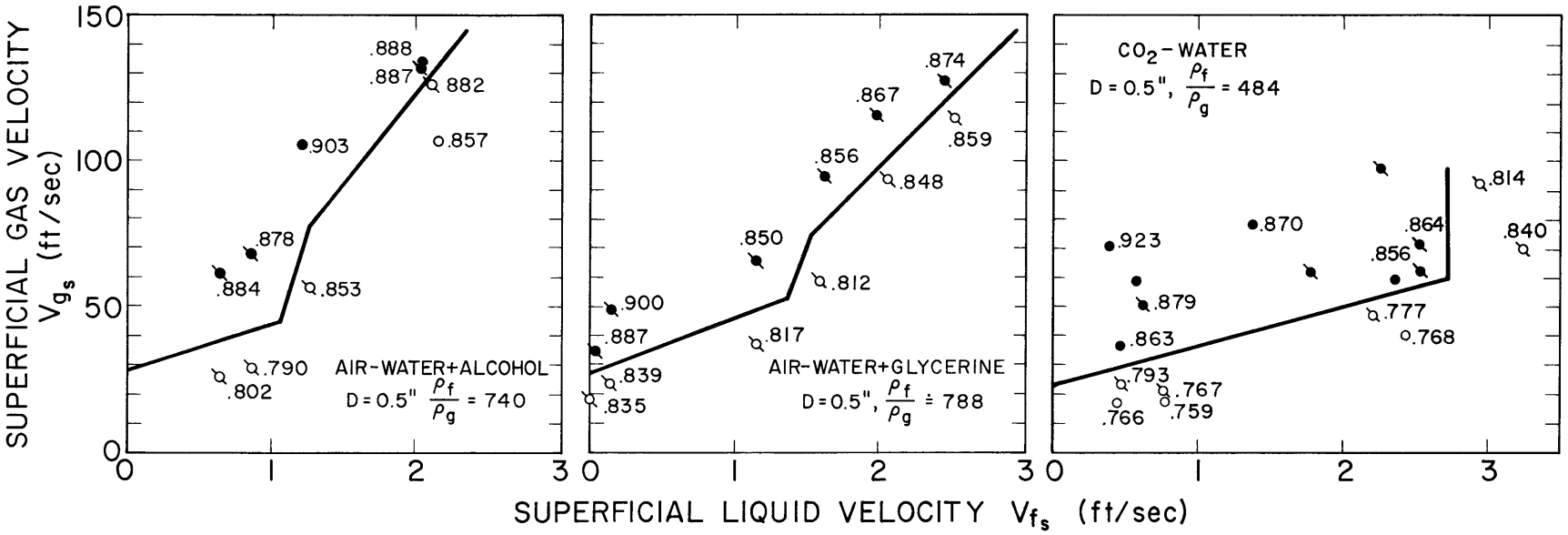

FIG. 9 FIG. 10 FIG. 11

FIGURES 9, 10, AND 11
TRANSITION LINES FOR 0.5" TUBE
TWO COMPONENTS

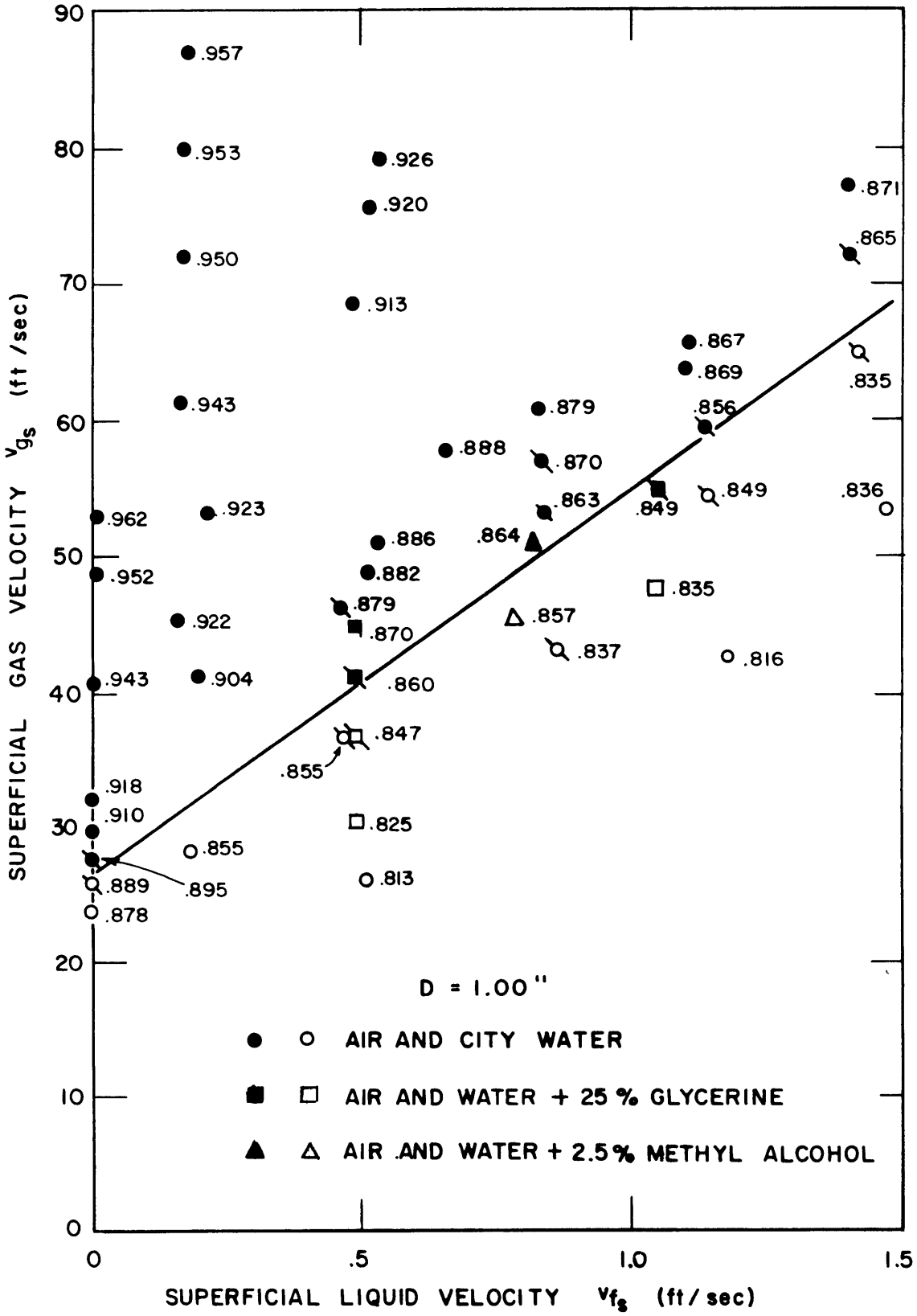

FIG. 12 TRANSITION LINE FOR AIR AND WATER (ETC.), 1.0" TUBE, ATMOSPHERIC PRESSURE.

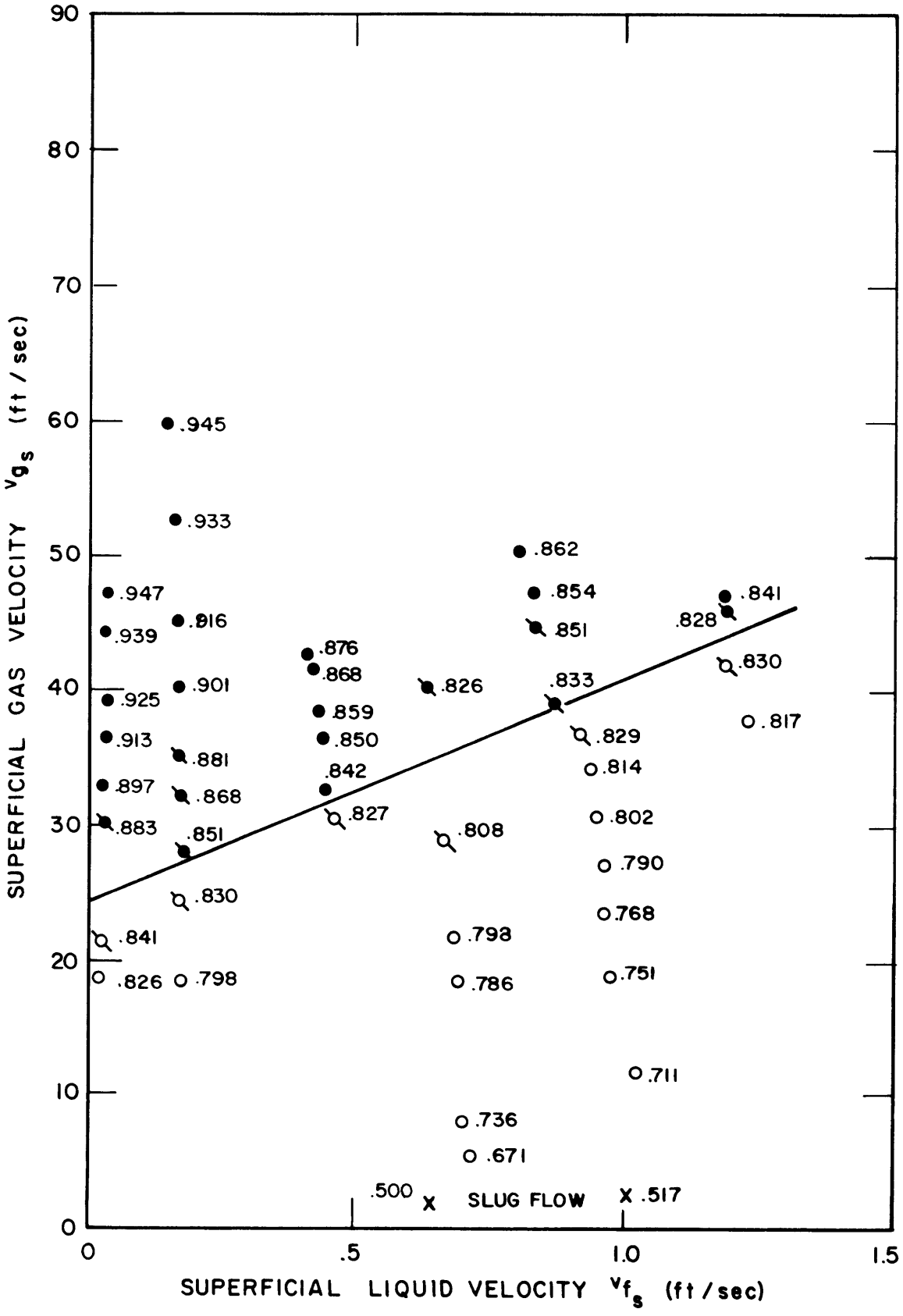

FIG. 13 TRANSITION LINE FOR AIR AND WATER, 1.5" TUBE, ATMOSPHERIC PRESSURE.

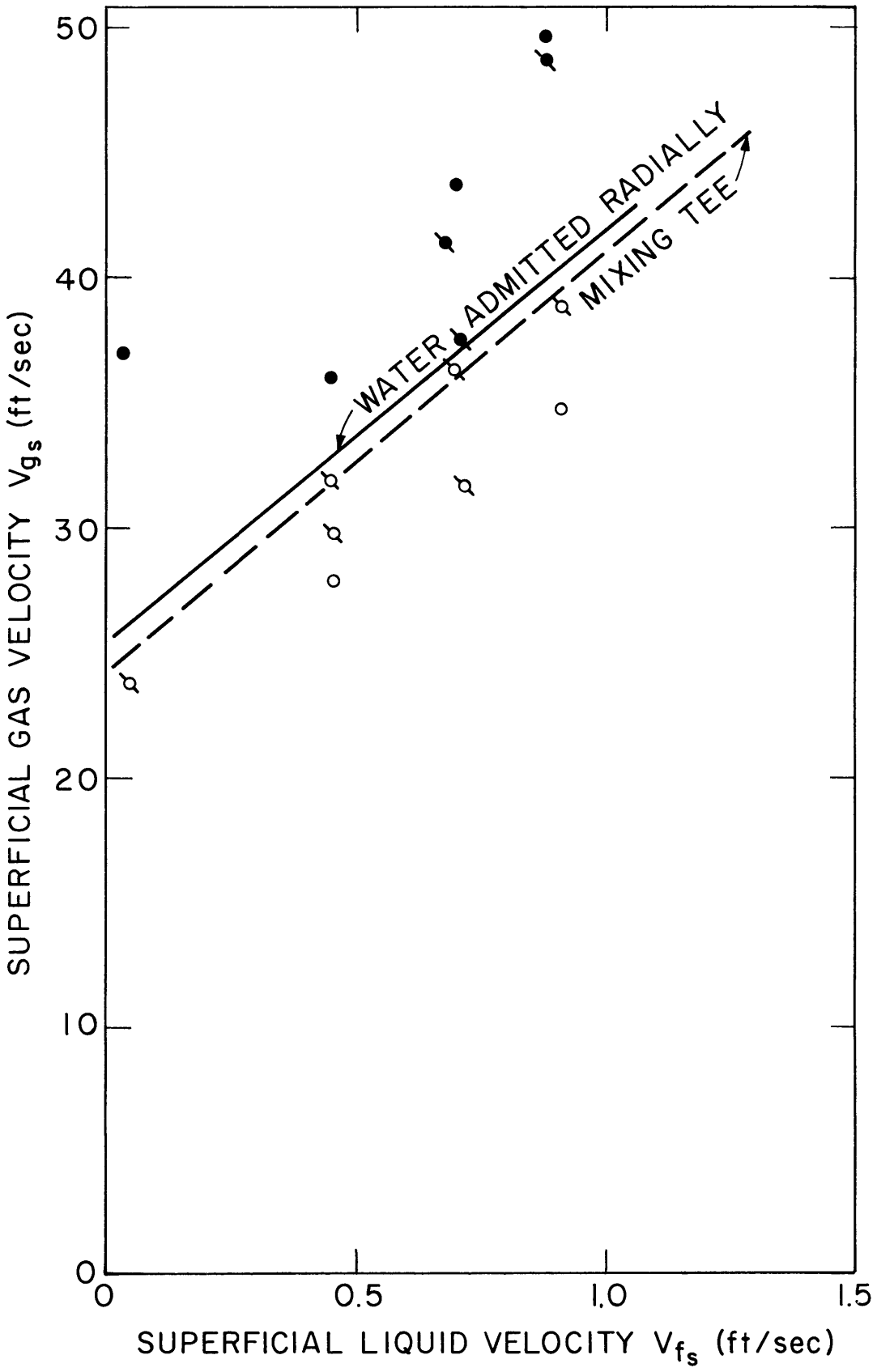

FIG. 13a D=1.5" AIR AND CITY WATER RADIAL ADMISSION OF WATER THROUGH HOLES IN TUBE WALL

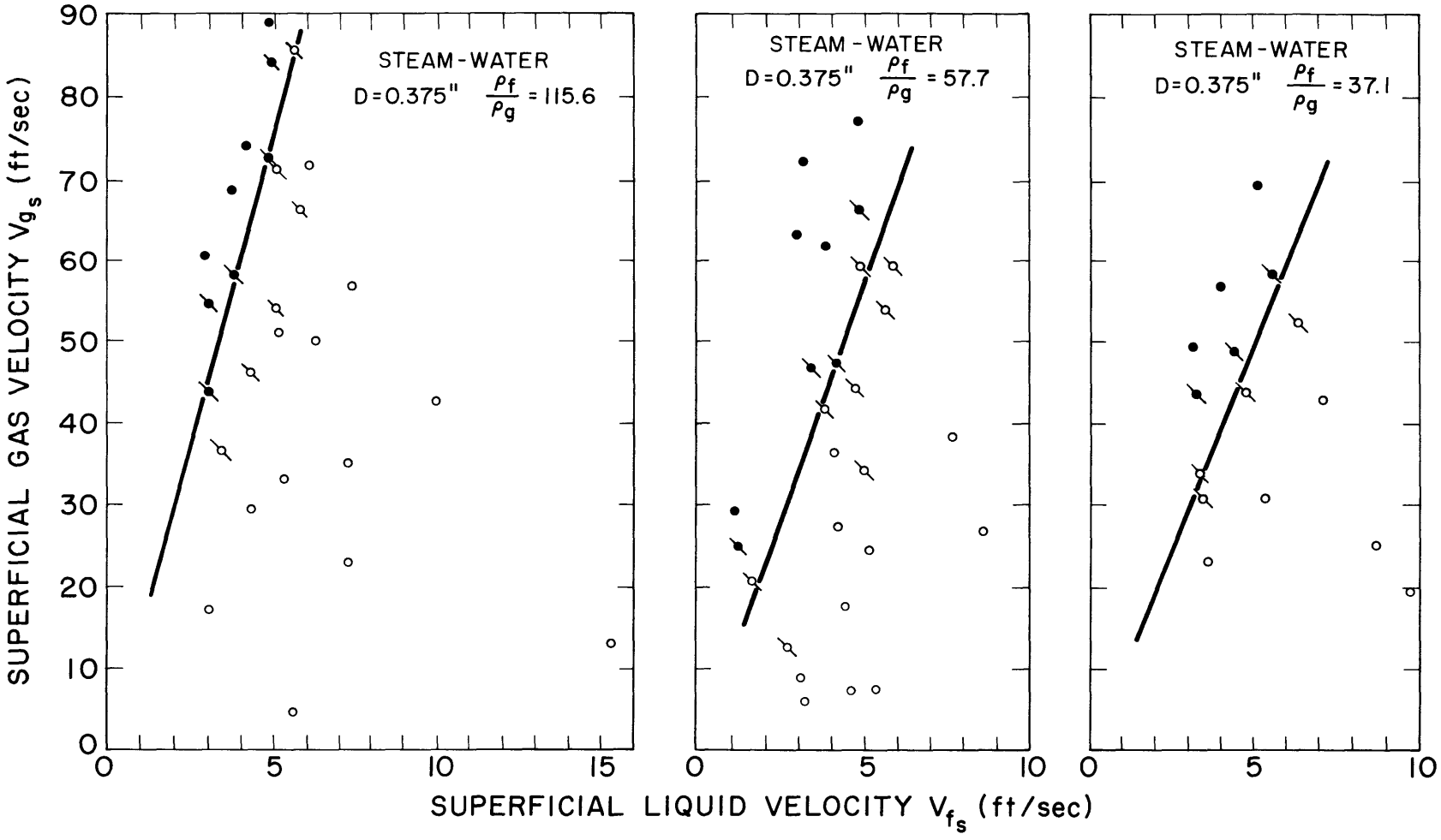

FIG. 14 FIG. 15 FIG. 16

FIGURES 14, 15, AND 16

TRANSITION LINES FOR STEAM AND WATER IN 0.375" TUBE AT 215, 415 AND 615 psia

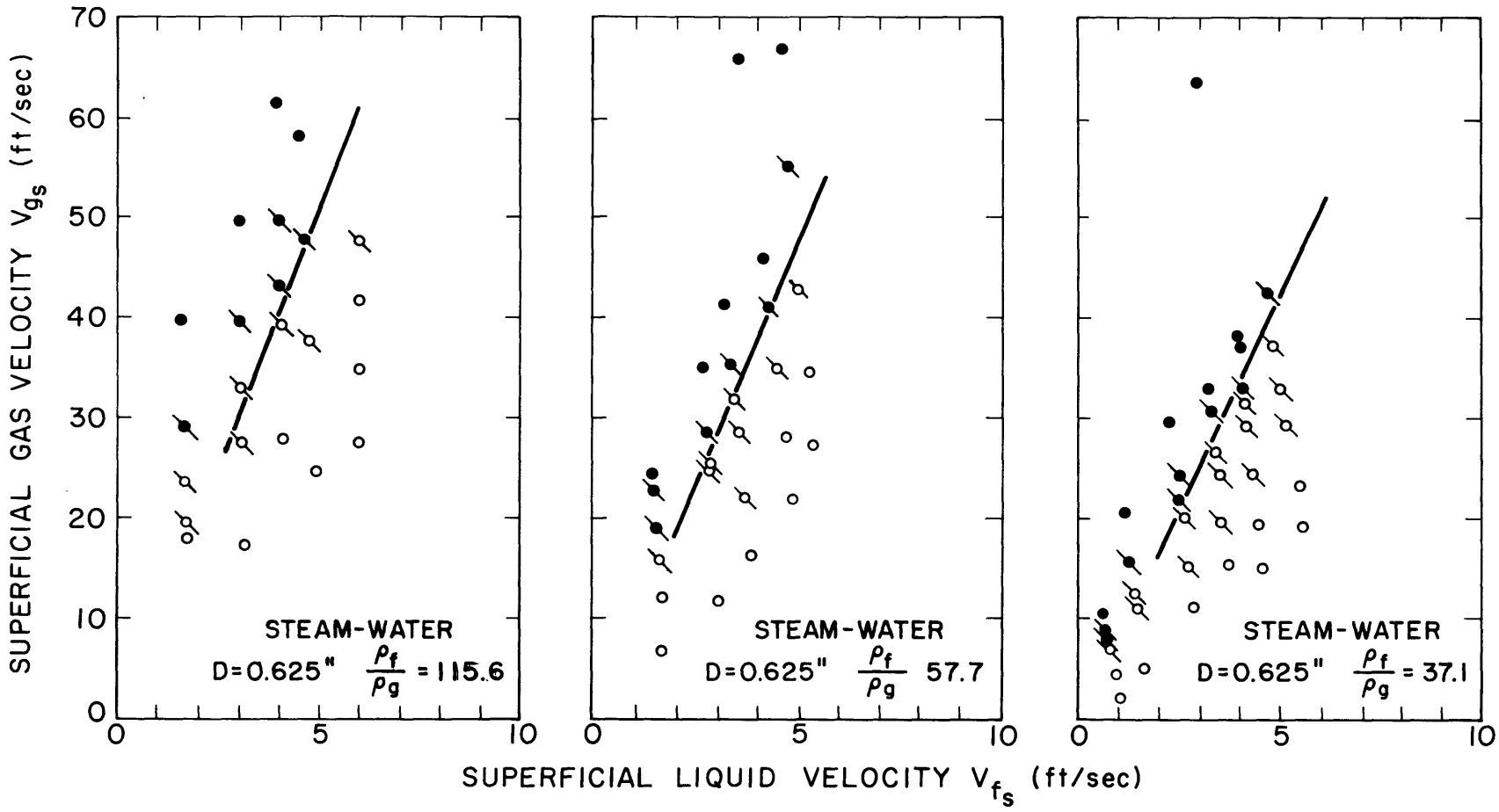

FIG. 17 FIG. 18 FIG. 19

FIGURES 17, 18, AND 19

TRANSITION LINES FOR STEAM AND WATER IN 0.625" TUBE AT 215, 415 AND 615 psia

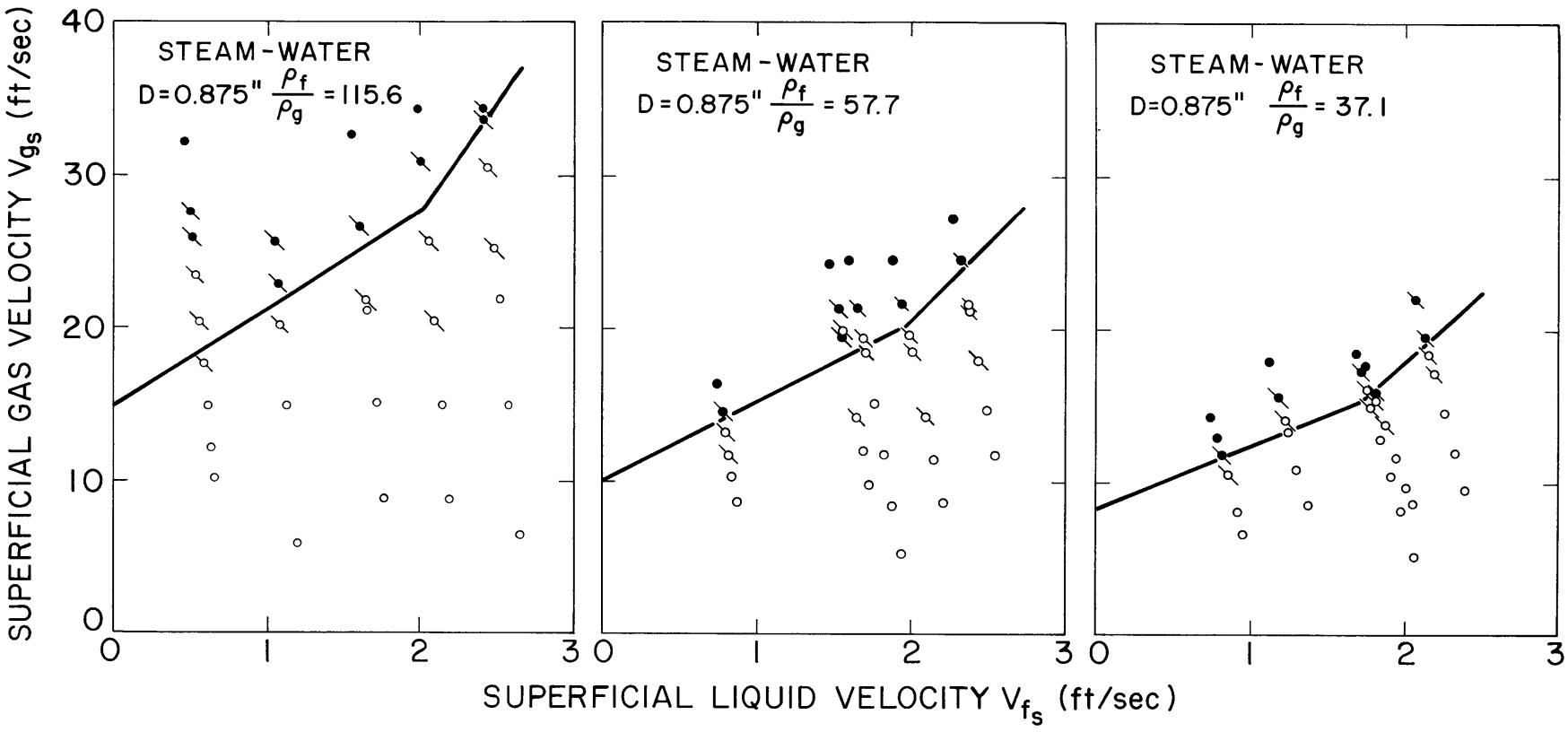

FIG. 20 FIG. 21 FIG. 22

FIGURES 20, 21, AND 22

TRANSITION LINES FOR STEAM AND WATER IN 0.875" TUBE AT 215, 415, AND 615 psia

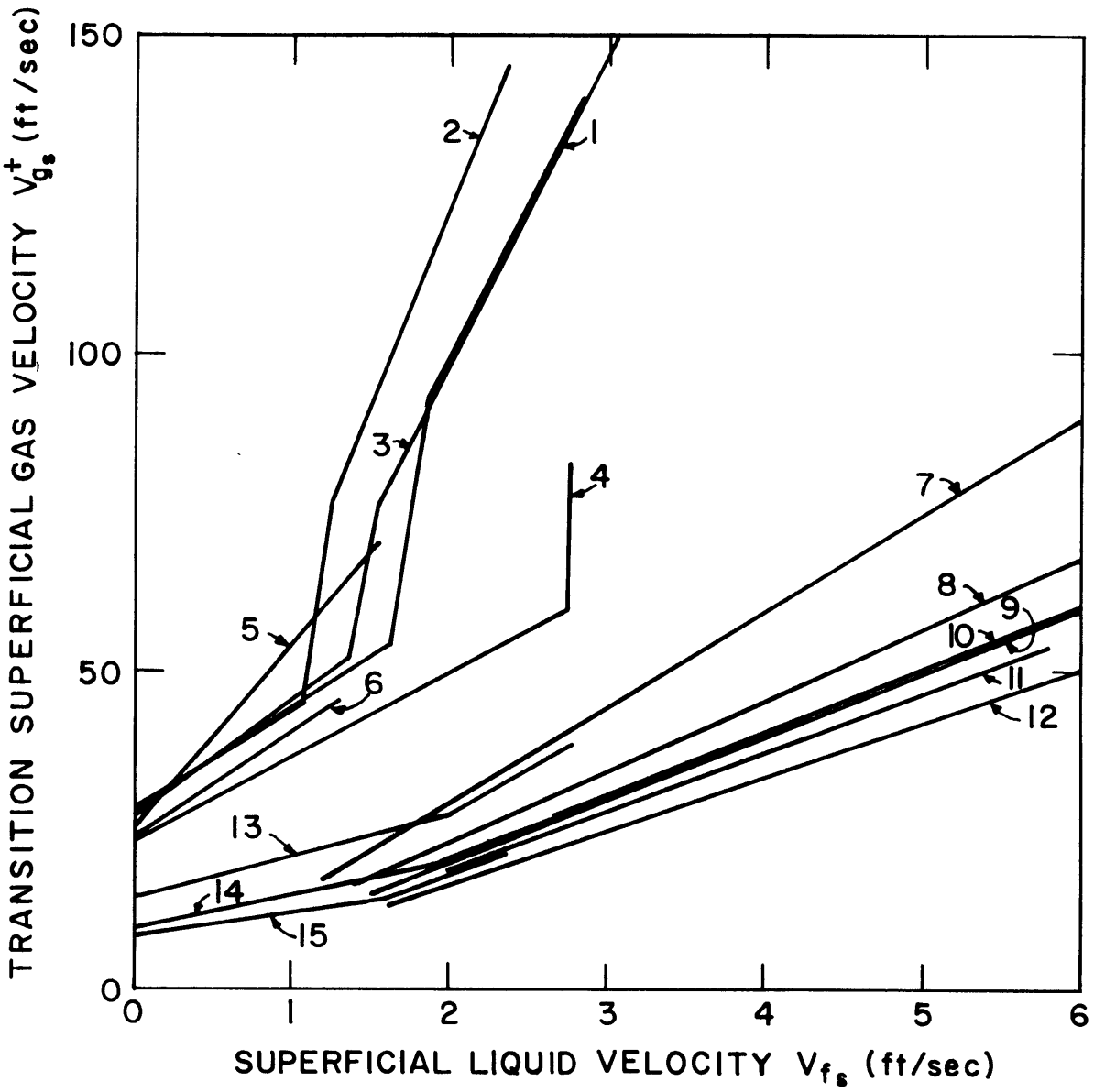

FIGURE 23
ANNULAR–SEMIANNULAR TRANSITION LINES FOR VARIOUS PIPES AND FLUIDS

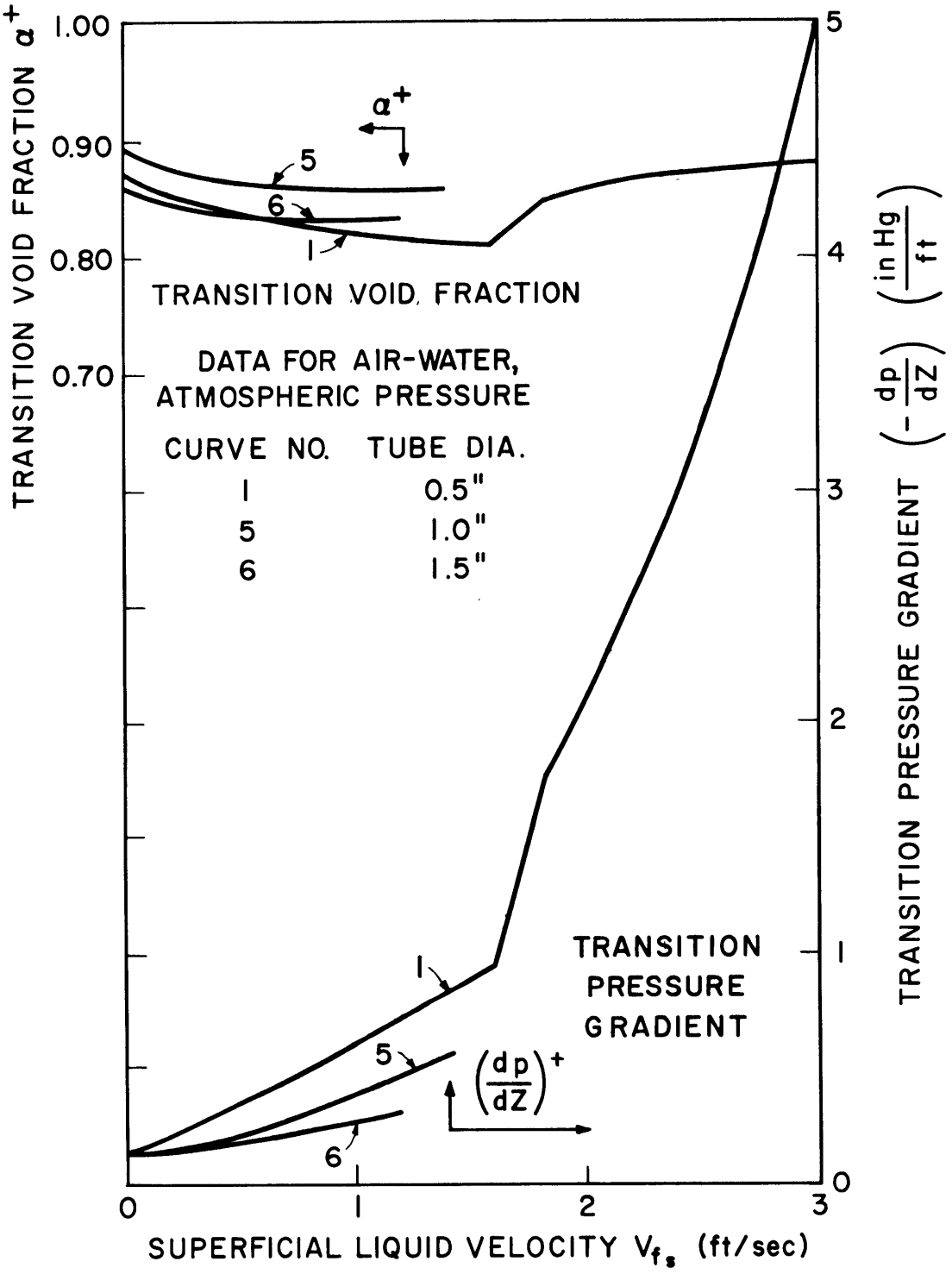

FIGURE 24
TRANSITION VOID AND PRESSURE DROP FOR AIR-WATER TESTS

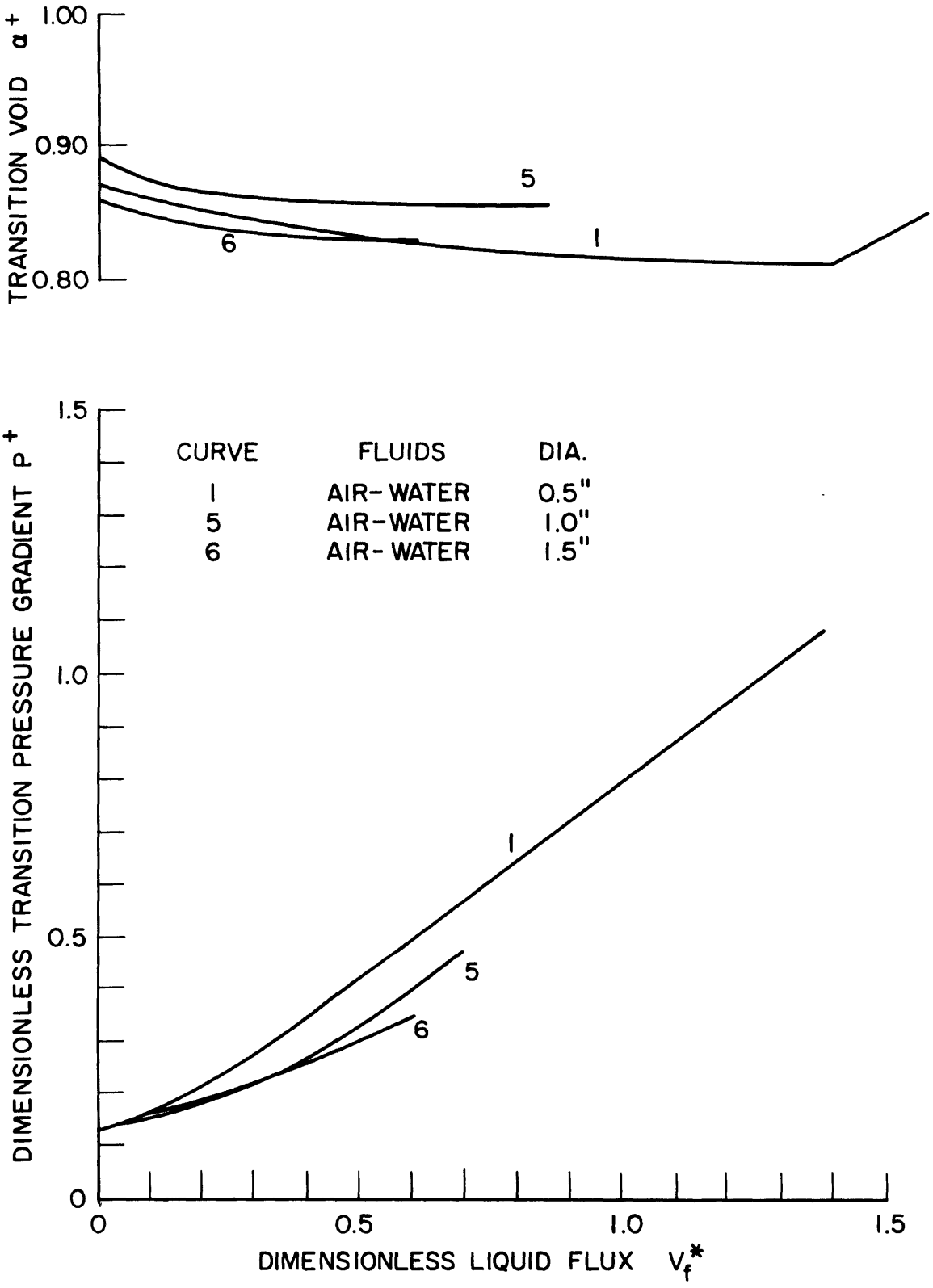

FIGURE 24a TRANSITION VOID AND DIMENSIONLESS PRESSURE DROP VS. V_f^*

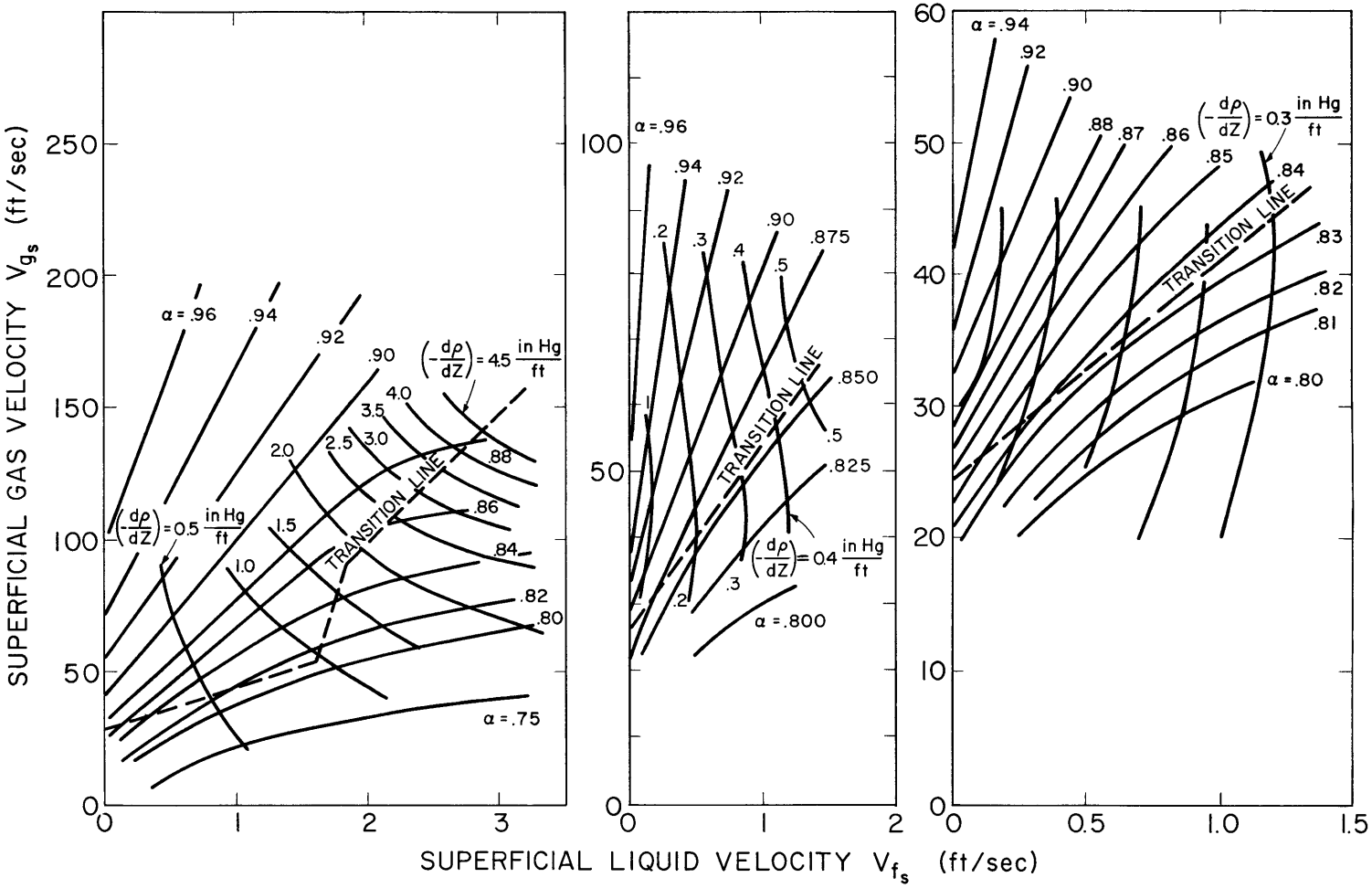

FIG. 25 FIG. 26 FIG. 27

FIGURES 25, 26, AND 27
VOID FRACTION AND PRESSURE GRADIENT FOR
AIR AND WATER IN 0.5," 1.0," AND 1.5" TUBES

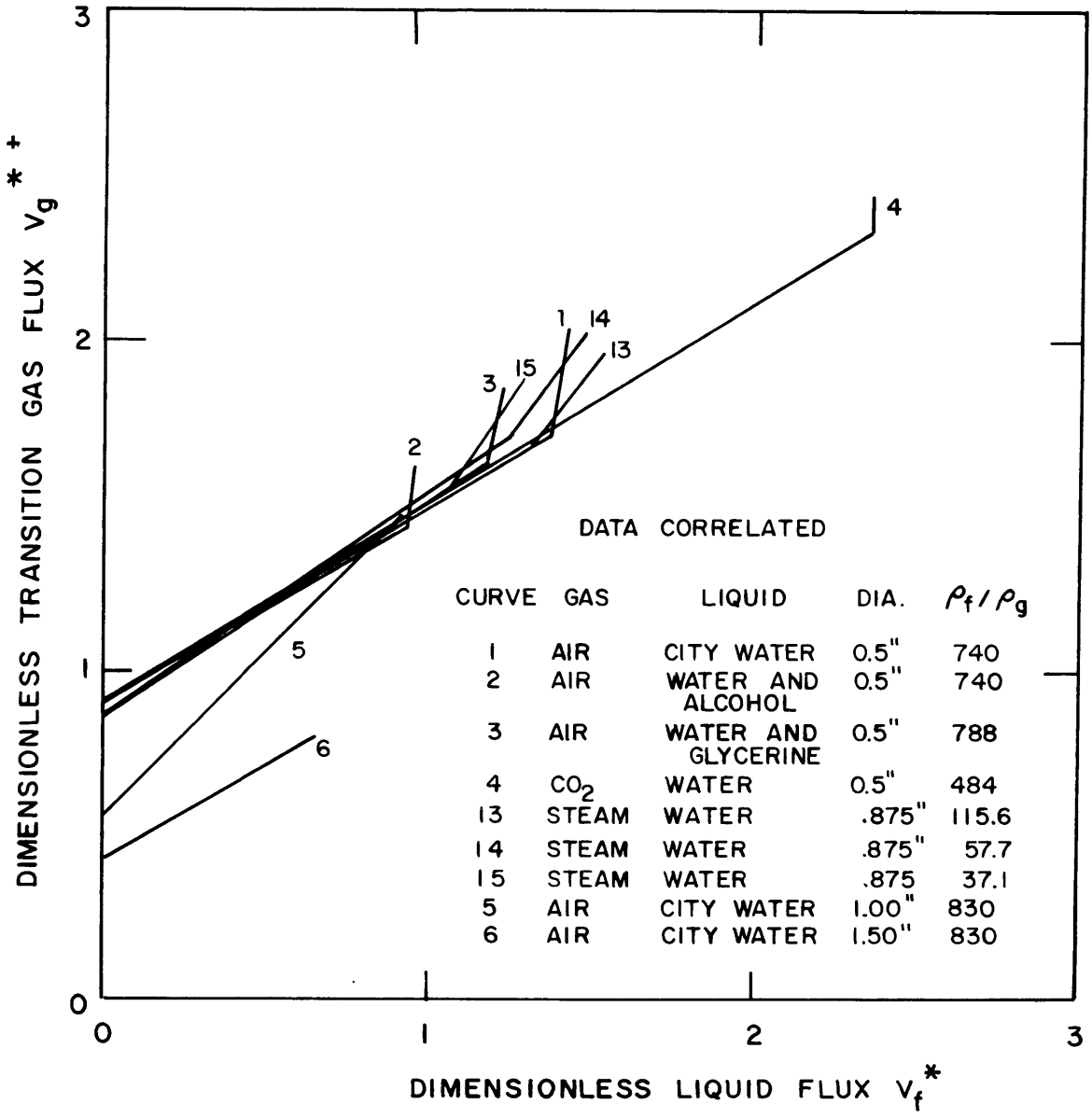

FIG. 28 ANNULAR-SEMIANNULAR TRANSITION LINE FOR LOW LIQUID FLUX

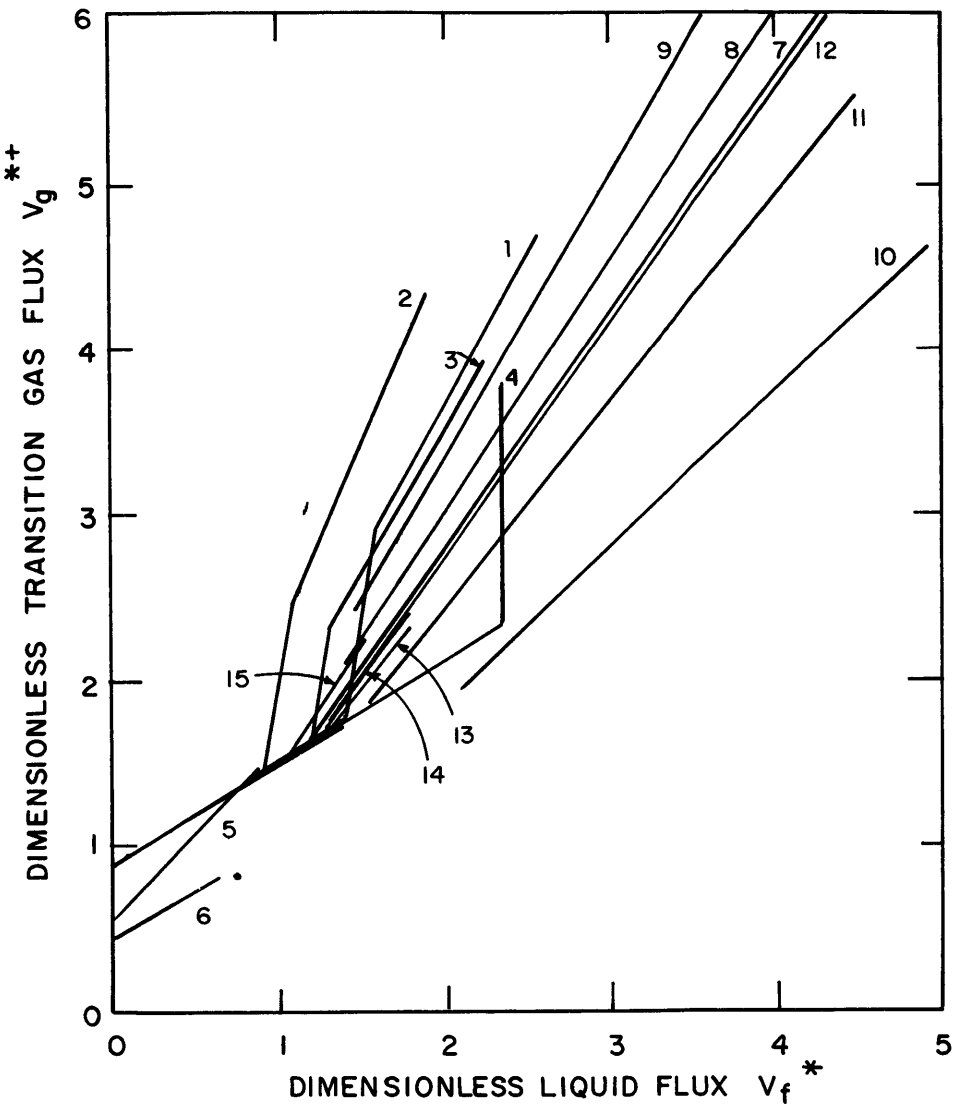

FIG. 29 TRANSITION LINES FOR HIGH LIQUID FLOW (DIMENSIONLESS COORDINATES)

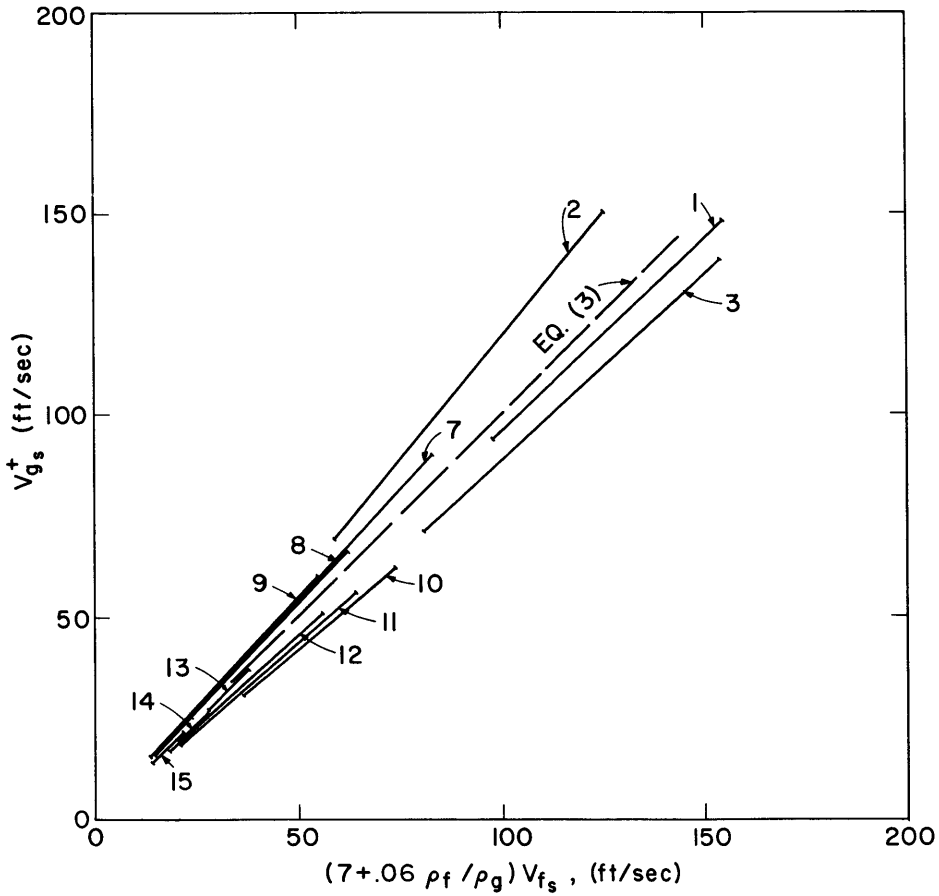

FIG. 29a ANNULAR-SEMIANNULAR TRANSITION LINE FOR HIGH LIQUID FLOW

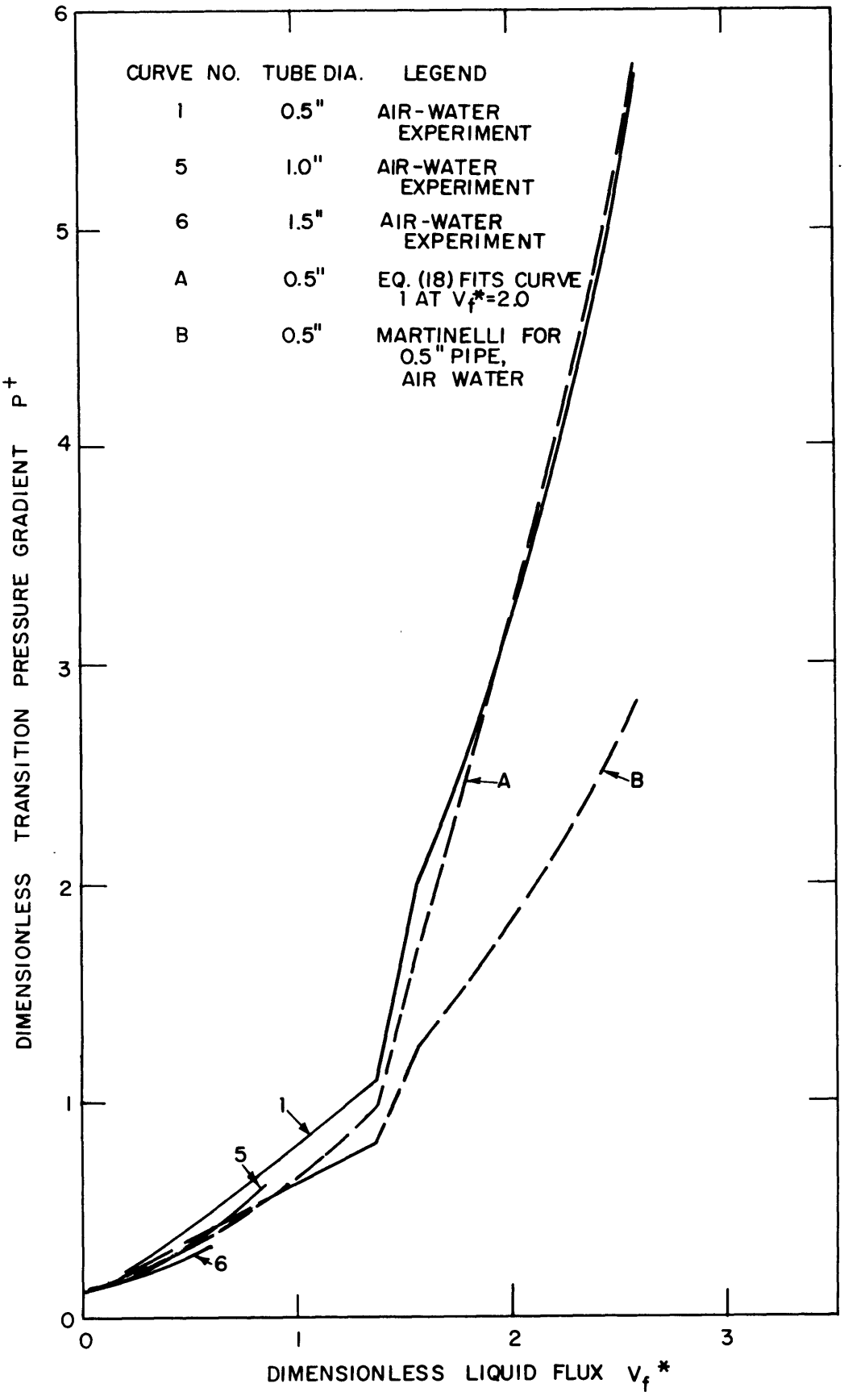

FIG 30 DIMENSIONLESS PRESSURE GRADIENT AT TRANSITION

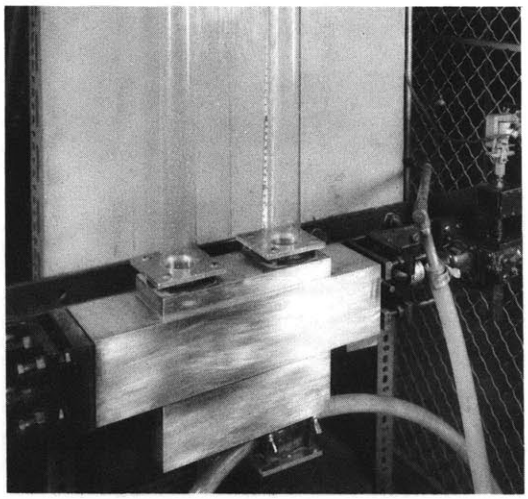

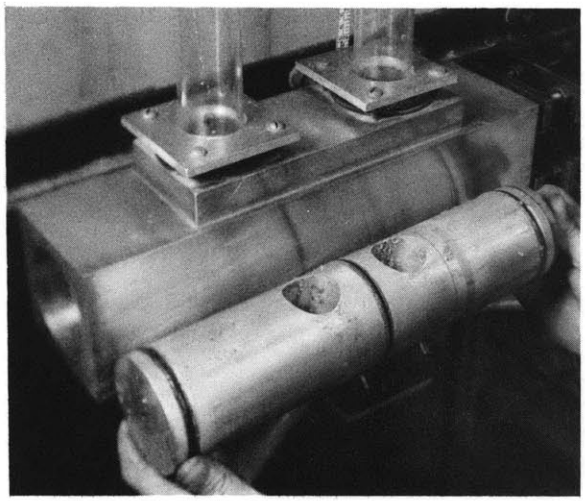

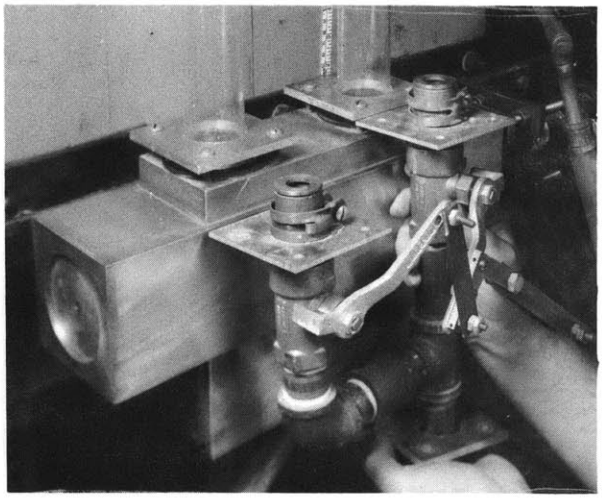

FIGURE 31

QUICK-ACTING VALVES

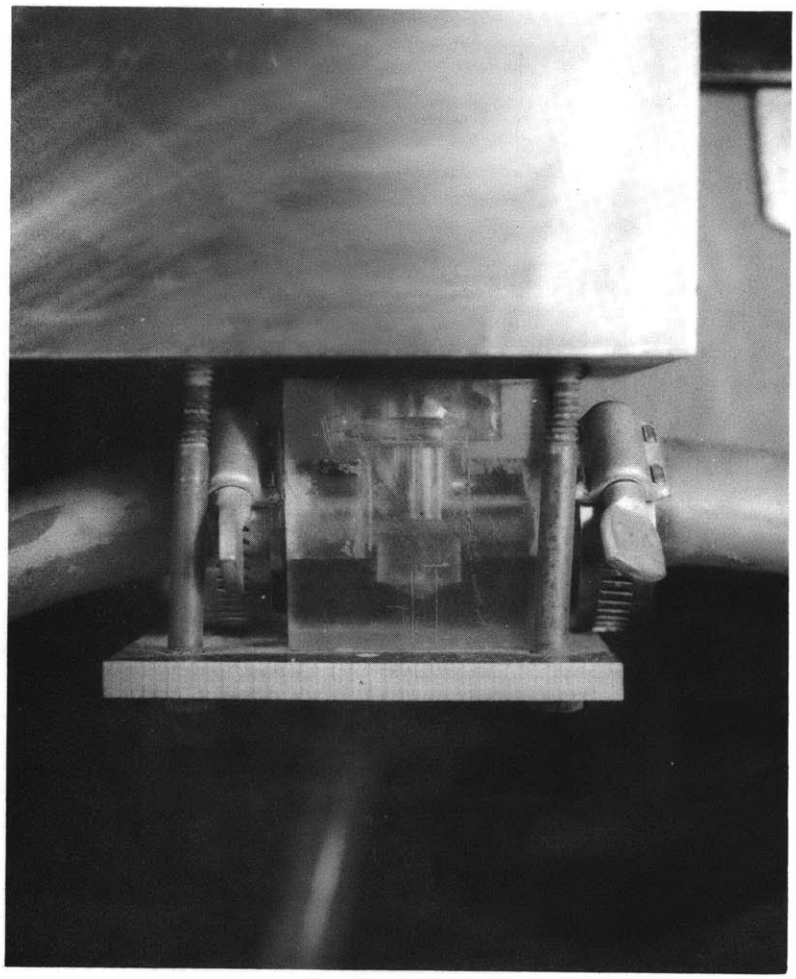

FIGURE 32
MIXING TEE